



Review

Paeoniae Radix Alba and Network Pharmacology Approach for Osteoarthritis: A Review

Bo Wang^{1,2} , Changcai Bai^{1,2,*}  and Yuanyuan Zhang^{3,*}

¹ College of Pharmacy, Ningxia Medical University, No. 1160 Sheng-Li Street, Yinchuan 750004, China; wangking1126@163.com

² Key Laboratory of Ningxia Ethnomedicine Modernization, Ministry of Education, Ningxia Medical University, Yinchuan 750004, China

³ School of Chinese Materia Medica, Beijing University of Chinese Medicine, Beijing 102488, China

* Correspondence: changcaibai@163.com (C.B.); zyy10101@126.com (Y.Z.)

Abstract: Osteoarthritis (OA) is the most common type of arthritis and affects more than 240 million people worldwide; the most frequently affected areas are the hips, knees, feet, and hands. OA pathophysiology is multifactorial, involving genetic, developmental, metabolic, traumatic, and inflammation factors. Therefore, treatments able to address several path mechanisms can help control OA. Network pharmacology is developing as a next-generation research strategy to shift the paradigm of drug discovery from “one drug, one target” to “multi-component, multi-target”. In this paper, network pharmacology is employed to investigate the potential role of *Paeoniae Radix Alba* (PRA) in the treatment of OA. PRA is a natural product known for its protective effects against OA, which has recently drawn attention because of its ability to provide physiological benefits with fewer toxic effects. This review highlights the anti-inflammatory properties of PRA in treating OA. PRA can be used alone or in combination with conventional therapies to enhance their effectiveness and reduce side effects. The study also demonstrates the use of network pharmacology as a cost-effective and time-saving method for predicting therapeutic targets of PRA in OA treatment.

Keywords: immune-inflammatory; osteoarthritis; *Paeoniae Radix Alba*; network pharmacology



Citation: Wang, B.; Bai, C.; Zhang, Y. *Paeoniae Radix Alba* and Network Pharmacology Approach for Osteoarthritis: A Review. *Separations* **2024**, *11*, 184. <https://doi.org/10.3390/separations11060184>

Academic Editor: Xiumei Li

Received: 9 May 2024

Revised: 3 June 2024

Accepted: 7 June 2024

Published: 12 June 2024



Copyright: © 2024 by the authors. Licensee MDPI, Basel, Switzerland. This article is an open access article distributed under the terms and conditions of the Creative Commons Attribution (CC BY) license (<https://creativecommons.org/licenses/by/4.0/>).

1. Introduction

Osteoarthritis (OA) is the top common joint disease and medical concern in the world, with loss of articular cartilage and changes in subchondral bone, menisci, synovium, ligaments, nerves, and periarticular muscle. OA can lead to joint pain, cartilage damage and degeneration, synovial inflammation, and swelling, which seriously affects the patient’s quality of life and is a health burden for families and society [1,2]. Currently, although Western medicine, such as oral therapy [3], intra-articular injection [4], rehabilitation exercise [5], and surgery [6], treatments for OA are available, they all focus on alleviating the clinical symptoms rather than treating the underlying causes. Therefore, it is critical to discover non-invasive treatments that are efficient in alleviating chronic pain, restoring joint function, and reducing side effects in OA patients. Given the complicated pathological mechanism of OA, including neovascularization, subjection to hypoxia, mechanical stress, and inflammation, novel drugs may need to target multiple pathways simultaneously [7,8].

For this reason, natural products with various chemical ingredients and numerous target characteristics have attracted wide attention as alternative therapies for OA. It is estimated that by 2050, there will be USD 5 trillion spent worldwide on medicinal plants, up from the current USD 14 billion yearly [9]. Traditional Chinese Medicine (TCM) has a history of 2300 years in treating various diseases with natural products with few adverse effects and has attracted more advertece in recent years. The natural product artemisinin being found to help treat malaria is a prime example. Radix *Paeoniae Alba* (aka PRA) is the dried root of *Paeonia lactiflora* Pall (PLP), a plant belonging to the Ranunculaceae family.

The plant is primarily distributed in the temperate regions of the world, especially in South China, Korea, and Japan. PRA is a TCM with the functions of nourishing blood, preventing perspiration, regulating menstruation, extinguishing liver wind, and has astringent and analgesic characteristics. It is widely used in China and other Asian countries and was first listed as a medicine in *Sheng Nong's Herbal Classic* [10,11]. The primary representative ingredients in PRA contain flavonoids [12], monoterpenes [13], and triterpenes [14]. Modern research has substantiated the analgesic, immunoregulatory, and anti-inflammatory properties of PRA [15,16]. Previous research shows that PRA alone or in combination with other herbs impacts OA [17]. Nevertheless, there is still a lack of adequate research focused on the treatment of OA by PRA [18,19], and its mechanism of action remains to be answered.

Utilizing improvements in bioinformatics and related databases, network pharmacology integrates technologies and contents from multiple disciplines, such as pharmacology, bioinformatics, and computer science, and discovers the interrelationship between drug–target–pathway–disease, which presents novel ideas and methods for the in-depth study of TCM.

In the present study, given the network pharmacology approach, we aimed to explore the primary bioactive constituents of PRA and predict their effective molecular targets and potential mechanisms in the treatment of OA by using network pharmacology, gene ontology (GO), and the Kyoto Encyclopedia of Genes and Genomes (KEGG) functional enrichment. Our investigation can help to understand the potential role of PRA in the treatment of OA and provide a reference for subsequent drug development and clinical application.

2. Materials and Methods

2.1. Screening and Target Prediction of Active Components of PRA

All of the candidate ingredients of PRA were retrieved using the Traditional Chinese Medicine Systems Pharmacology Database and Analysis Platform (<https://old.tcmsp-e.com/tcmsp.php>, accessed on 31 May 2022) [20], which is a platform based on the medicinal herbs repository comprehensive information network of chemicals, targets, and affiliated drug targets, including the pharmacokinetic properties of natural compounds like oral bioavailability (OB), drug-likeness (DL), intestinal epithelial permeability, blood–brain barrier penetrability, and water solubility. We applied candidate components that match both $OB \geq 30\%$ and $DL \geq 0.18$ as an evaluation criterion, using pharmacodynamics for further exploration.

2.2. Collection of PRA-Related Targets

The molecular structures of the 13 active components were evaluated and acquired in standard SMILES format from the PubChem database (<https://pubchem.ncbi.nlm.nih.gov/>, accessed on 31 May 2022) [21]. Chem Draw Ultra 8.0 was used to create the 2D chemical structures of potential candidate components. To gather the active components and possible targets of PRA, we searched the Swiss Target Prediction web tool (<http://www.swisstargetprediction.ch/>, accessed on 31 May 2022) to supplement predicted protein targets with the potential candidate compounds [22]. The specific information for the Swiss Target Prediction was used to extract the conventional SMILES, with the species “Homo sapiens” as the target organism. The target information was then gathered and collated using Microsoft Excel software. Simultaneously, the UniProt database (<https://www.uniprot.org/>, accessed on 31 May 2022) [23] was utilized to standardize the pharmacological target within each primary substance, which was limited to the “human species”.

2.3. Screening of Disease-Related Targets

The keyword “osteoarthritis” was searched from OMIM [24]. Gene Cards (<https://www.genecards.org/>, accessed on 31 May 2022) [25], Drug Bank (<https://go.drugbank.com/>, accessed on 31 May 2022) [26], and PharmGKB database (<https://www.pharmgkb.org/>, accessed on 31 May 2022) [27] are comprehensive databases to obtain OA-related target

gene information. In addition, a Microsoft Excel program (Microsoft Office 2019) was applied to eliminate redundant genes to avoid duplicates.

2.4. Protein–Protein Interaction (PPI) Network Construction and Screening of Core Targets

The Veeny 2.1 overlap (<https://bioinfo.gp.cnb.csic.es/tools/venny/>, accessed on 31 May 2022) was created to acquire and evaluate the targets of potential active components in PRA and the disease-related gene of OA. The PPI network regulates all organisms' appropriate functions. The STRING database (https://cn.stringdb.org/cgi/input?sessionId=b4jyCOBi5KO&input_page_show_search=on, accessed on 31 May 2022) [28] was used to erect the PPI network to elucidate the interaction of therapeutic target genes and the central gene, with "Homo sapiens" being determined and presented in Cytoscape 3.9.1 software [29]. Only PPI data with an association highest score of more than 0.4 (medium confidence) were set for protein–protein interaction for topology analysis. The degree of a node in the PPI network refers to the number of other nodes with apparent connections. The degrees and total scores of pertinent protein nodes were exported and saved as TSV format files after unnecessary protein nodes were removed in a bid to obtain protein–protein interactions. The data were imported into Cytoscape 3.9.1 software for further analysis of PPI network topology. The central targets are the top 10 targets based on the values computed using network analysis (Cytoscape plugin). Therefore, a node's importance in a PPI network increases with degree.

2.5. GO and KEGG Pathway Enrichment Analysis

GO terms are classified into 3 aspects, namely, biological process (BP), cellular component (CC), and molecular function (MF). GO and KEGG pathway enrichment analyses were performed in this investigation using the Metascape platform (<https://metascape.org/gp/index.html#/main/step1>, accessed on 31 May 2022) [30], which includes an extensive annotation function and gene annotation data that are updated regularly. For analysis of the results, the bioinformatic web platform (<http://www.bioinformatics.com.cn/?p=1>, accessed on 31 May 2022) showed the GO keywords and KEGG pathways sorted by the *p*-value and count for visual analysis [20].

2.6. Molecular Docking Imitation of Active Compound

Molecular docking technology is used in network pharmacology to verify compound targets, predict the molecules' relationship of binding mode and affinity, and also research the interaction between molecules. It is a standard method to discover novel drugs [21]. The 2D structure of the small molecule ligands for the 8 representative compounds were first obtained from the PubChem online database (<https://pubchem.ncbi.nlm.nih.gov/>, accessed on 31 May 2022) as small molecule ligand files for molecular docking. The 3D structure file of the core target protein receptor was acquired from the PDB online database (<https://www.rcsb.org>, accessed on 31 May 2022). The ligand and protein obtained for molecular docking were prepared using AutoDock Vina software (<http://vina.scripps.edu/>). The core target protein's crystal structure was processed, including removal of hydrogenation, modification of amino acids, optimization of energy, and adjustment of force field parameters, and then met the low-energy conformation of the ligand structure. Finally, the target structure was docked with the active component structure using the internal vina of PyRx-Virtual Screening software. The Affinity (kcal/mol) value represents the binding capacity of the representative ingredient and target; the lower the binding capacity, the more stable the binding between the ligand and the receptor.

3. Network Pharmacology: A Multi-Target and Multi-Component Strategy

In 2007, Andrew L. Hopkins made the initial proposal for the field of network pharmacology [22]. Polypharmacology and system biology are combined in network pharmacology to address the limited effectiveness of selective single-target medications [23]. Systems biology involves studying biological structures and processes by developing mathematical

formulas and models that explain how a system operates in response to specific gene or protein changes. Network pharmacology, viewed as an emerging paradigm in pharmacological research, complements systems biology by offering insights into pharmacological and disease targets, along with their molecular pathways, from extensive datasets [24]. Nowadays, network pharmacology is increasingly used to study the overall pharmacological effects of drugs on diseases and their therapeutic mechanisms [25]. Various databases are essential for network research. Examples include Swiss Target and Pub Chem for active components, KEGG and DAVID for pathway enrichment, and STRING for drug molecule information. BIND and DIP are crucial for biomolecular interactions, while HPRD and BioGRID provide protein-related data. Moreover, OMIM and DisGeNET are valuable for disease target retrieval. To analyze these data, researchers often utilize Cytoscape for network creation and analysis [26]. Network pharmacology, with its multi-component, multi-target approach, has the potential to address the limitations of single-target therapies and facilitate the discovery of new medications for various diseases, including OA.

4. Extraction and Purification Process of Compounds

When terpenes are extracted from PRA, methanol and ethanol are the most often employed solvents. At present, the total glucosides of paeony (TGP) is thought to be PRA's primary active ingredient. TGP is hydrophilic monoterpene glycosides typically extracted using water or alcohol. Extraction from PRA can be carried out through methods like ethanol/water reflux, ultrasonic, and microwave-assisted extraction. The initial TGP extract contains impurities such as tannins and carbohydrates, necessitating purification for high-purity TGP. Common purification methods include clarification, organic solvent extraction, and microporous resin purification [27,28]. Researchers have optimized the TGP extraction processes using techniques like response surface methods. For instance, optimal conditions are a solid ratio of 9 mL/g, two extractions with 85% ethanol, each lasting 100 min [29]. In addition, the most used technique for separating analytes from PRA is ultrasonication. Shen et al. extracted PRA for 40 min using an ultrasonic extraction method with 70% (v/v) ethanol, yielding a single standard material for eleven components [30]. In one investigation, 50% acetonitrile demonstrated the highest reflux-based extraction effectiveness of albiflorin and paeoniflorin when compared to solutions including water, 50% ethanol, 50% methanol, and acetonitrile at different concentrations. A 2-h reflux period was also required [31]. Wang et al. fractionated the preparative purification of paeoniflorin and albiflorin from the rhizome of *Paeonia lactiflora* Pall (PLP) using macroporous resins [32]. Paeoniflorin, albiflorin, benzoyl paeoniflorin, and benzoyl albiflorin were separated from the 50% ethanol extract of PRA using a D101 macroporous resin column [33]. At present, research has focused on developing greener and more efficient methods for extracting and purifying TGP from PRA. For instance, a method that has shown promise involves subcritical water extraction followed by purification using macroporous resin. In this optimal extraction process, the time duration is 22 min, the extraction temperature is 158 °C, the solid ratio is 21 mL/g, and the maximum extraction rate of TGP using subcritical water extraction can reach 7.08% [34].

5. Analysis of Chemical Compounds

Due to advancements in chemical component separation and analysis technologies, an increasing number of new components in PRA can now be separated and analyzed. With the aid of highly sensitive and selective MS detectors, LC-MS has emerged as a superior technique for analyzing trace compounds in compounds with low UV absorption or PRA, when compared to UV detectors. According to earlier studies [35], 26 major ingredients in *Paeoniae Radix Rubra* (PRR) were identified using LC coupled with DAD and time-of-flight (TOF) MS. Fingerprint analysis, a widely used method in the discriminate analysis of PRA, offers a comprehensive view of the chemical compositions of herbal medicines. Infrared spectroscopy (IR) provides physical properties and chemical composition information, facilitating a more thorough evaluation of TCM quality. Wang et al. reported the

difference between PRA and PRR by IR [36]. Furthermore, various spectral techniques, including Raman spectroscopy and X-ray diffraction spectroscopy, have been utilized in the discrimination analysis of PRA. HPLC fingerprinting has emerged as a robust method for investigating chemical variances among species and geographical regions. In HPLC analyses of monoterpene glycosides and polyphenols, reverse-phase chromatography is commonly employed, with ODS (C₁₈) often being the preferred stationary phase [27].

6. Anti-OA Effects

Inflammation is a sophisticated process arising from the host's defense system response to different internal and external stimuli, which typically occur in various tissues and organs [37]. Chronic inflammation is regarded as a significant factor in various health conditions, such as rheumatoid arthritis [38] and asthma [39]. Therefore, suppressing inflammation is essential for treating diseases associated with chronic inflammation. The identification of new anti-inflammatory drugs from natural sources has increasingly garnered interest in the field of medical research. In recent decades, numerous publications have detailed the diverse biological activities of the *Paeonia* in both in vitro and in vivo experimental models. These activities include anti-inflammatory [40], antioxidant [41], antibacterial [42], antiviral [43], anti-tumor [44], central nervous system protective [45], and cardiovascular protective effects [46]. Currently, the anti-inflammatory properties of the genus *Paeonia* have been extensively researched.

6.1. Crude Extracts

In a rat model of arthritis induced by Complete Freund's Adjuvant, PRA extract demonstrated a reduction in inflammation associated with arthritis. Administered at doses of 10 mg of PRA per gram of body weight, the swelling inhibition rates were 58.2%, 50.48%, and 35.67% at 3 h, 6 h, and 15 h, respectively. At the medium dosage, swelling inhibition percentages were 50.82%, 50.05%, and 35.39%, while at intermediate and low dosages, the inhibition percentages were 33.78%, 39.56%, and 28.66%, respectively. The decrease in phosphodiesterase (PDE) activity in neutrophils and possibly other inflammatory cells may play a role in mediating this anti-inflammatory impact [47].

6.2. Pure Compounds

Liao et al. conducted a series of studies of the anti-OA activity and mechanism of action of TGP [48]. In vivo and in vitro experiments demonstrated that TGP had a protective effect on cartilage. Treatment with TGP could induce the synthesis of critical elements in the cartilage extracellular matrix and downregulate the synthesis of degrading enzymes in the extracellular matrix. Regarding the underlying mechanisms, TGP inhibited the phosphorylation and nuclear translocation of p65 by regulating the nuclear factor-kappa B (NF- κ B) signaling pathway. In addition, TGP could reduce the secretion of IL-1 β , IL-6, and tumor necrosis factor- α (TNF- α). Moreover, it has a sustained effect on coupled subchondral bone remodeling through regulation of the OPG/RANKL/RANK pathway. Further investigation showed that TGP may protect articular cartilage by downregulating the NF- κ B signaling pathway and may support coupled subchondral bone remodeling by regulating the OPG/RANKL/RANK signaling pathway in the DMM-induced KOA model of mouse for OA treatment. Another study suggests that paeoniflorin could inhibit IL-1 β -induced MMP secretion via the NF- κ B pathway in chondrocytes, exerting anti-OA effects [49]. Hu et al. found that paeoniflorin may exert its protective effect by inhibiting IL-1 β -induced chondrocyte apoptosis by regulating the Bax/Bcl-2/caspase-3 signaling pathway [50]. In one study, paeoniflorin shows chondroprotective effects under IL-1 β stress by regulating the circ-PREX1/miR-140-3p/WNT5B axis [51]. Furthermore, paeoniflorin inhibited the production of nitric oxide and prostaglandin E2 induced by IL-1 β and the expression of inducible nitric oxide synthase and cyclooxygenase-2 in chondrocytes. The NF- κ B transcription factors play a prominent role in various pathways and mediators influencing the occurrence of OA. IL-1 β may activate NF- κ B by triggering the degradation

of $I\kappa B\alpha$, which leads to the translocation of NF- κ B p65 from the cytoplasm to the nucleus, thereby regulating the expression of various inflammation-related genes. Treatment with paeoniflorin reduced the expression of NF- κ B p65 and $I\kappa B\alpha$ degradation induced by IL-1 β in OA chondrocytes. This therapeutic effect may occur through modulation of NF- κ B signaling pathway [52].

Based on our research of the literature on published reviews [48,53], extracts and compounds of the PRA exhibit a broad spectrum of anti-OA activity and have multiple targets of action. Among the components of the extracts, monoterpene glycosides are the main active compounds. The plant extract TGP has been used clinically in the treatment of inflammatory diseases [54]. TGP has good efficacy and few side effects in rheumatoid arthritis patients but produces slow therapeutic effects [55]. Currently, TGP is often used in combination with other drugs to treat autoimmune diseases, but there are few pharmacological reports on this topic.

7. Coupling of Network Pharmacology with PRA in OA Diseases

7.1. Screening of Candidate Ingredients of PRA

The TCMSP was screened, and 85 components of PRA were identified. According to the filtering criteria of $OB \geq 30\%$ and $DL \geq 0.18$, 13 active compounds were identified that satisfied the criteria (Table 1). The 13 active constituents of PRA contained 11 α ,12 α -epoxy-3 β -23-dihydroxy-30-norolean-20-en-28,12 β -olide, paeoniflorgenone, (3S,5R,8R,9R,10S,14S)-3,17-dihydroxy-4,4,8,10,14-pentamethyl-2,3,5,6,7,9-hexahydro-1H-cyclopenta[a]phenanthrene-15,16-dione (DPHCD), lactiflorin, paeoniflorin, paeoniflorin_qt, albiflorin_qt, benzoyl paeoniflorin, Mairin, beta-sitosterol, sitosterol, kaempferol, and (+)-catechin, extracted through TCMSP.

7.2. Potential Target Genes and the PPI Network Map of PRA Therapy for OA

A total of 3493 OA target genes, excluding duplicates, were determined through investigations of the GeneCard, OMIM, Drug Bank, and PharmGKB databases. For the 13 active components of PRA, 707 target genes were retrieved from the TCMSP database and Swiss Target Prediction (Supplementary Table S1). Upon verification, duplicates were discarded, yielding 406 target genes. Using the Venny 2.1 program, OA target genes and PRA target genes were intersected to obtain 232 candidate targets (Figure 1A) (Table 2). The PPI network map was created by sequentially importing the 232 target genes into the STRING database (Figure 1B). The network was visualized and explored by evaluating centrality and other variables using the Cytoscape program. Following these guidelines, all of the targets were organized into circles.

Table 1. Characteristics of active ingredients in PRA.

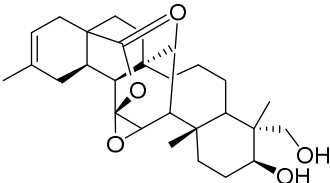
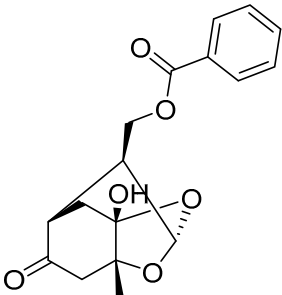
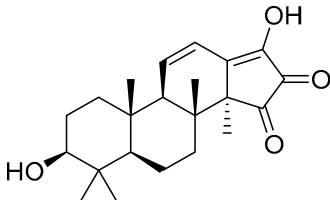
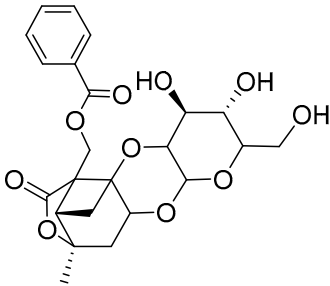
No	Mol ID	Compound	Molecular Structure	Molecular Weight	AlogP	Hdon	Hacc	OB (%)	DL	HL
1	MOL001910	11 α ,12 α -epoxy-3 β -23-dihydroxy-30-norolean-20-en-28,12 β -olide		470.71	3.91	2	5	64.77	0.4	2.62
2	MOL001918	Paeoniflorgenone		318.35	0.79	1	6	87.59	0.4	7.45
3	MOL001919	DPHCD		358.52	2.69	2	4	43.56	0.5	4.34
4	MOL001921	Lactiflorin		462.49	-0.57	3	10	49.12	0.8	7.26

Table 1. Cont.

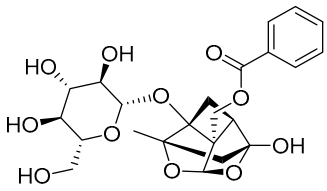
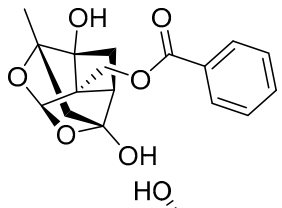
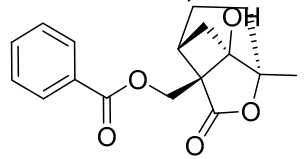
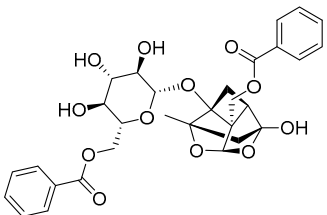
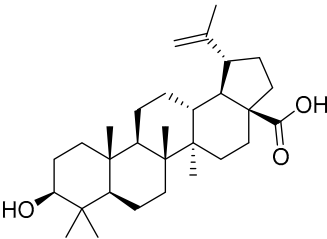
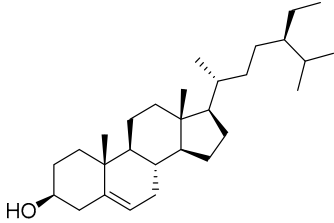
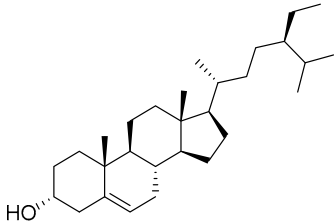
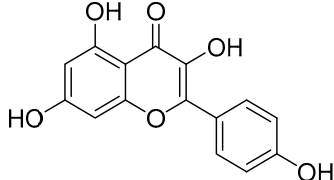
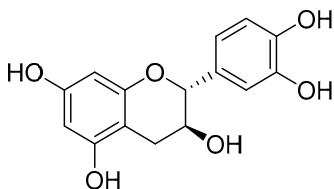
No	Mol ID	Compound	Molecular Structure	Molecular Weight	AlogP	Hdon	Hacc	OB (%)	DL	HL
5	MOL001924	Paeoniflorin		480.51	-1.28	5	11	53.87	0.8	13.9
6	MOL001925	paeoniflorin_qt		318.35	0.46	2	6	68.18	0.4	8.81
7	MOL001928	albiflorin_qt		318.35	0.42	2	6	66.64	0.3	6.54
8	MOL001930	benzoyl paeoniflorin		584.62	0.81	4	12	31.27	0.8	-1.9
9	MOL000211	Mairin		456.78	6.52	2	3	55.38	0.8	8.87

Table 1. Cont.

No	Mol ID	Compound	Molecular Structure	Molecular Weight	AlogP	Hdon	Hacc	OB (%)	DL	HL
10	MOL000358	beta-sitosterol		414.79	8.08	1	1	36.91	0.8	5.36
11	MOL000359	Sitosterol		414.79	8.08	1	1	36.91	0.8	5.37
12	MOL000422	Kaempferol		286.25	1.77	4	6	41.88	0.2	14.7
13	MOL000492	(+)-catechin		290.29	1.92	5	6	54.83	0.2	0.61

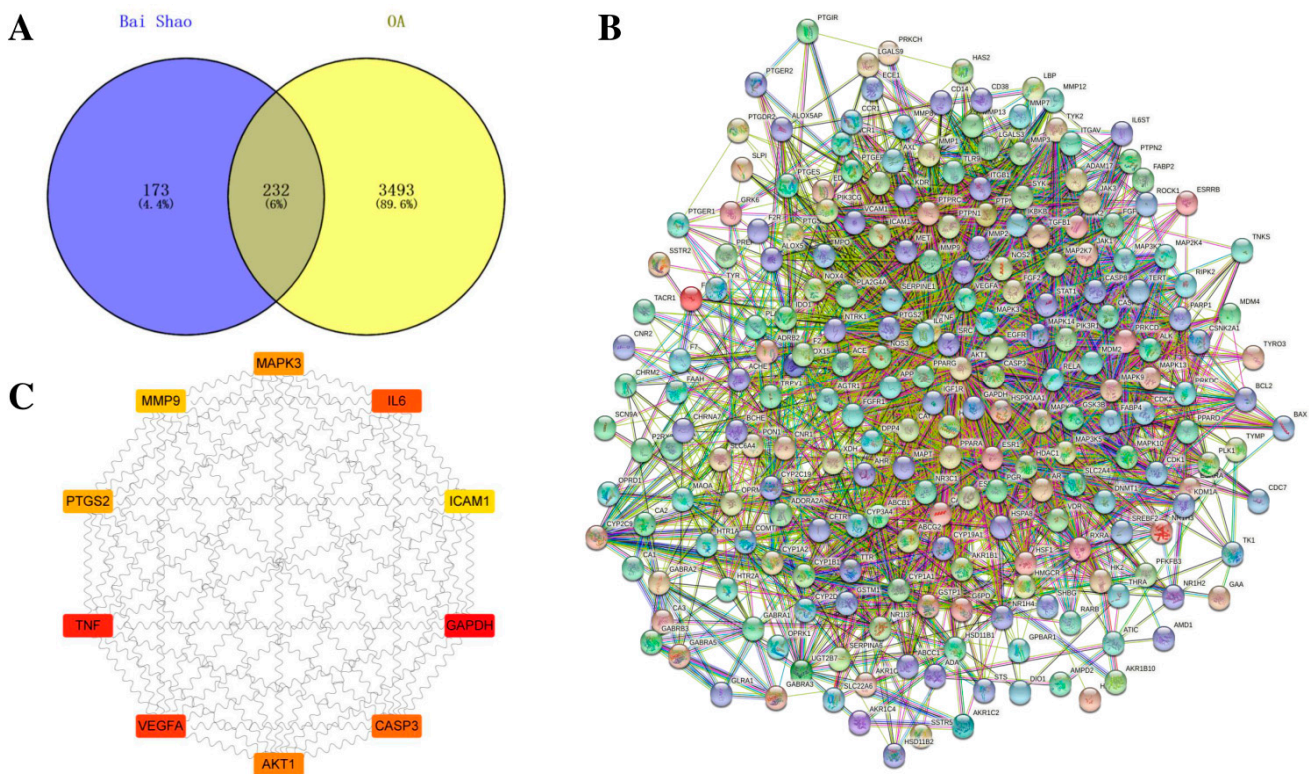


Figure 1. The results of potential target genes of PRA therapy for OA. (A) Ven diagram of OA and PRA intersection targets; (B) 232 targets related to OA were utilized to construct the PPI network; (C) The top 10 targets ranked by degree value were identified as the kernel targets.

Table 2. 232 potential target genes of PRA therapy for OA.

NO	Target	Symbol	NO	Target	Symbol
1	Gamma-aminobutyric acid receptor subunit alpha-1	GABRA1	117	Insulin-like growth factor I receptor	IGF1R
2	Progesterone receptor	PGR	118	Tyrosine-protein kinase SRC	SRC
3	Androgen Receptor	AR	119	Vascular endothelial growth factor receptor 2	KDR
4	Cytochrome P450 19A1	CYP19A1	120	MAP kinase p38 alpha	MAPK14
5	Testis-specific androgen-binding protein	SHBG	121	Peroxisome proliferator-activated receptor gamma	PPARG
6	Glucocorticoid receptor	NR3C1	122	Thrombin	F2
7	Estrogen receptor alpha	ESR1	123	Nitric-oxide synthase, endothelial	NOS3
8	Tyrosine-protein kinase JAK1	JAK1	124	Coagulation factor VII	F7
9	Tyrosine-protein kinase JAK2	JAK2	125	Transcription factor p65	RELA
10	Vanilloid receptor	TRPV1	126	Inhibitor of nuclear factor kappa-B kinase subunit beta	IKBKB
11	Cytochrome P450 2D6	CYP2D6	127	RAC-alpha	AKT1
12	Cytochrome P450 2C9	CYP2C9	128	serine/threonine-protein kinase	TNF
13	Tyrosine-protein kinase JAK3	JAK3	129	Tumor necrosis factor	XDH
14	Tyrosine-protein kinase TYK2	TYK2	130	Xanthine dehydrogenase/oxidase	MMP1
15	Delta opioid receptor (by homology)	OPRD1	131	Interstitial collagenase	STAT1
16	Kappa Opioid receptor (by homology)	OPRK1	132	Signal transducer and activator of transcription 1-alpha/beta	HMOX1
17	Serotonin 1a (5-HT1a) receptor	HTR1A	133	Heme oxygenase 1	CYP3A4
18	Steryl-sulfatase	STS	134	Cytochrome P450 3A4	CYP1A2
19	Poly [ADP-ribose] polymerase-1	PARP1	135	CYP1A2	CYP1A1
20	c-Jun N-terminal kinase 1	MAPK8	136	Cytochrome P450 1A1	ICAM1
21	Glycogen synthase kinase-3 beta	GSK3B	137	Intercellular adhesion molecule 1	SELE
22	c-Jun N-terminal kinase 3	MAPK10	138	E-selectin	VCAM1
23	Dual specificity mitogen-activated protein kinase kinase 4	MAP2K4	139	Vascular cell adhesion protein 1	CYP1B1
24	MAP kinase p38 delta	MAPK13	140	Cytochrome P450 1B1	ALOX5
25	Cyclin-dependent kinase 2/cyclin A	CDK2	141	Arachidonate 5-lipoxygenase	HAS2
26	Dual specificity mitogen-activated protein kinase kinase 7	MAP2K7	142	Hyaluronan synthase 2	GSTP1
				Glutathione S-transferase P	

Table 2. Cont.

NO	Target	Symbol	NO	Target	Symbol
27	c-Jun N-terminal kinase 2	MAPK9	143	Aryl hydrocarbon receptor	AHR
28	CDC7	CDC7	144	Solute carrier family 2, facilitated glucose transporter member 4	SLC2A4
29	Interleukin-6 receptor subunit beta	IL6ST	145	Type I iodothyronine deiodinase	DIO1
30	Estrogen receptor beta	ESR2	146	Glutathione S-transferase Mu 1	GSTM1
31	Catechol O-methyltransferase	COMT	147	Antileukoproteinase	SLPI
32	C-C chemokine receptor type 1	CCR1	148	NADPH oxidase 4	NOX4
33	Estrogen-related receptor alpha	ESRRA	149	Aldose reductase (by homology)	AKR1B1
34	Estrogen-related receptor beta	ESRRB	150	Tyrosinase	TYR
35	Serine/threonine-protein kinase RIPK2	RIPK2	151	Multidrug resistance-associated protein 1	ABCC1
36	Muscarinic acetylcholine receptor M2	CHRM2	152	P-glycoprotein 1	ABCB1
37	Thyroid hormone receptor alpha	THRA	153	ATP-binding cassette sub-family G member 2	ABCG2
38	Dipeptidyl peptidase IV	DPP4	154	Monoamine oxidase A	MAOA
39	Endothelin receptor ET-A (by homology)	EDNRA	155	Tyrosine-protein kinase SYK	SYK
40	Thrombin and coagulation factor X	F10	156	Matrix metalloproteinase 9	MMP9
41	Cyclin-dependent kinase 1	CDK1	157	Matrix metalloproteinase 2	MMP2
42	Carbonic anhydrase II	CA2	158	Arachidonate 15-lipoxygenase	ALOX15
43	Carbonic anhydrase I	CA1	159	Adenosine A2a receptor (by homology)	ADORA2A
44	P2X purinoceptor 3	P2RX3	160	Transthyretin	TTR
45	GABA-A receptor; alpha-3/beta-3/gamma-2	GABRB3	161	Tankyrase-2	TNKS
46	GABA-A receptor; alpha-2/beta-3/gamma-2	GABRA2	162	Casein kinase II alpha	CSNK2A1
47	Mitogen-activated protein kinase kinase 5	MAP3K5	163	Epidermal growth factor receptor erbB1	EGFR
48	Cannabinoid receptor 2	CNR2	164	Myeloperoxidase	MPO
49	TYRO3	TYRO3	165	PI3-kinase p85-alpha subunit	PIK3R1
50	Type-1 angiotensin II receptor (by homology)	AGTR1	166	Focal adhesion kinase 1	PTK2
51	DNA-dependent protein kinase	PRKDC	167	Matrix metalloproteinase 13	MMP13
52	Cannabinoid receptor 1	CNR1	168	Matrix metalloproteinase 3	MMP3
53	Rho-associated protein kinase 1	ROCK1	169	Carbonic anhydrase III	CA3
54	Sodium channel protein type Ix alpha subunit	SCN9A	170	Serine/threonine-protein kinase PLK1	PLK1
55	Lysine-specific histone demethylase 1	KDM1A	171	Hepatocyte growth factor receptor	MET
56	Telomerase reverse transcriptase	TERT	172	Interleukin-8 receptor A	CXCR1
57	Protein-tyrosine phosphatase 2C	PTPN11	173	CaM kinase II beta	CAMK2B
58	Toll-like receptor (TLR7/TLR9)	TLR9	174	Tyrosine-protein kinase receptor UFO	AXL
59	Heat shock factor protein 1	HSF1	175	Aldo-keto reductase family 1 member C2 (by homology)	AKR1C2
60	Nerve growth factor receptor Trk-A	NTRK1	176	Aldo-keto reductase family 1 member C1 (by homology)	AKR1C1
61	Protein kinase C delta	PRKCD	177	Aldo-keto reductase family 1 member C4 (by homology)	AKR1C4
62	Prostaglandin G/H synthase 1	PTGS1	178	Beta-amyloid A4 protein	APP
63	Prostaglandin G/H synthase 2	PTGS2	179	Matrix metalloproteinase 12	MMP12
64	Phosphatidylinositol-4,5-bisphosphate 3-kinase catalytic subunit, gamma isoform	PIK3CG	180	CD38	CD38
65	5-hydroxytryptamine 2A receptor	HTR2A	181	Cystic fibrosis transmembrane conductance regulator	CFTR
66	Gamma-aminobutyric-acid receptor alpha-5 subunit	GABRA5	182	6-phosphofructo-2-kinase/fructose-2,6-bisphosphatase 3	PFKFB3
67	Gamma-aminobutyric-acid receptor alpha-3 subunit	GABRA3	183	G protein-coupled receptor kinase 6	GRK6
68	Beta-2 adrenergic receptor	ADRB2	184	Microtubule-associated protein tau	MAPT
69	Sodium-dependent serotonin transporter	SLC6A4	185	CAT	CAT
70	Mu-type opioid receptor	OPRM1	186	Bile acid receptor FXR	NR1H4
71	Neuronal acetylcholine receptor protein, alpha-7 chain	CHRNA7	187	G-protein coupled bile acid receptor 1	GPBAR1
72	Apoptosis regulator Bcl-2	BCL2	188	5-lipoxygenase activating protein	ALOX5AP
73	BAX	BAX	189	Fatty acid binding protein intestinal	FABP2
74	Caspase-9	CASP9	190	Anandamide amidohydrolase	FAAH
75	Caspase-3	CASP3	191	Solute carrier family 22 member 6 (by homology)	SLC22A6
76	Caspase-8	CASP8	192	Angiotensin-converting enzyme	ACE
77	Transforming growth factor beta-1	TGFB1	193	Retinoic acid receptor beta	RARB
78	Serum paraoxonase/arylesterase 1	PON1	194	Retinoid X receptor alpha	RXRA
79	HMG-CoA reductase	HMGCR	195	Cytosolic phospholipase A2	PLA2G4A
80	LXR-alpha	NR1H3	196	Integrin alpha-4/beta-1	ITGB1
81	Sterol regulatory element-binding protein 2	SREBF2	197	G protein-coupled receptor 44	PTGDR2
82	Cytochrome P450 2C19	CYP2C19	198	Integrin alpha-V/beta-3	ITGAV
83	Butyrylcholinesterase	BCHE	199	Leukocyte common antigen	PTPRC
84	Nuclear receptor ROR-alpha	RORA	200	Endothelin-converting enzyme 1	ECE1

Table 2. Cont.

NO	Target	Symbol	NO	Target	Symbol
85	Protein-tyrosine phosphatase 1B	PTPN1	201	AMP deaminase 2	AMPD2
86	Corticosteroid binding globulin	SERPINA6	202	Interleukin-6	IL6
87	Glucose-6-phosphate 1-dehydrogenase	G6PD	203	Monocyte differentiation antigen CD14	CD14
88	Nuclear receptor subfamily 1 group I member 3 (by homology)	NR1I3	204	Lipopolysaccharide-binding protein	LBP
89	Acetylcholinesterase	ACHE	205	Galectin-3	LGALS3
90	Vitamin D receptor	VDR	206	Galectin-9	LGALS9
91	LXR-beta	NR1H2	207	Heat shock protein HSP 90-alpha	HSP90AA1
92	Prostanoid EP1 receptor (by homology)	PTGER1	208	Somatostatin receptor 2	SSTR2
93	Prostanoid EP2 receptor (by homology)	PTGER2	209	Somatostatin receptor 1	SSTR1
94	11-beta-hydroxysteroid dehydrogenase 1	HSD11B1	210	Vascular endothelial growth factor A	VEGFA
95	Glycine receptor subunit alpha-1	GLRA1	211	Acidic fibroblast growth factor	FGF1
96	Peroxisome proliferator-activated receptor delta	PPARD	212	Basic fibroblast growth factor	FGF2
97	Nitric oxide synthase, inducible (by homology)	NOS2	213	Heparanase	HPSE
98	UDP-glucuronosyltransferase 2B7	UGT2B7	214	Plasminogen activator inhibitor-1	SERPINE1
99	11-beta-hydroxysteroid dehydrogenase 2	HSD11B2	215	Matrix metalloproteinase 7	MMP7
100	Prolyl endopeptidase	PREP	216	Matrix metalloproteinase 8	MMP8
101	Prostanoid EP4 receptor (by homology)	PTGER4	217	Beta-glucocerebrosidase	GBA
102	Indoleamine 2,3-dioxygenase	IDO1	218	Hexokinase type II	HK2
103	Protein Mdm4	MDM4	219	Histone deacetylase 1	HDAC1
104	p53-binding protein Mdm-2	MDM2	220	ADAM17	ADAM17
105	Prostanoid IP receptor	PTGIR	221	Somatostatin receptor 5	SSTR5
106	Fatty acid binding protein adipocyte	FABP4	222	Fibroblast growth factor receptor 1	FGFR1
107	Prostaglandin E synthase	PTGES	223	Glyceraldehyde-3-phosphate dehydrogenase liver	GAPDH
108	T-cell protein-tyrosine phosphatase	PTPN2	224	Lysosomal alpha-glucosidase	GAA
109	MAP kinase ERK1	MAPK3	225	Heat shock cognate 71 kDa protein DNA	HSPA8
110	Aldo-keto reductase family 1 member B10	AKR1B10	226	(cytosine-5)-methyltransferase 1	DNMT1
111	Phospholipase A2 group 1B	PLA2G1B	227	Adenosine deaminase	ADA
112	Protein kinase C eta	PRKCH	228	Mitogen-activated protein kinase kinase kinase 7	MAP3K7
113	Neurokinin 1 receptor (by homology)	TACR1	229	Thymidine kinase, cytosolic	TK1
114	Peroxisome proliferator-activated receptor alpha	PPARA	230	S-adenosylmethionine decarboxylase 1	AMD1
115	Proteinase-activated receptor 1	F2R	231	Thymidine phosphorylase	TYMP
116	ALK tyrosine kinase receptor	ALK	232	AICAR transformylase	ATIC

The Cytoscape software (a Cytoscape plugin) discovered and listed the top 10 potential genes closely related to PRA and OA from PPI network results (Figure 1C). These genes involve RAC-alpha serine/threonine-protein kinase (AKT1), caspase-3 (CASP3), glyceraldehyde-3-phosphate dehydrogenase liver (GAPDH), intercellular adhesion molecule 1 (ICAM1), interleukin-6 (IL-6), MAP kinase ERK1 (MAPK3), matrix metalloproteinase 9 (MMP9), prostaglandin G/H synthase2 (PTGS2), tumor necrosis factor (TNF), and vascular endothelial growth factor A (VEGFA).

7.3. Construction and Analysis of the PRA–OA–Potential Target Gene Network

To construct a PRA–OA–potential representative gene network, we must further input the data of Supplementary Table S1 and Table 2 into Cytoscape software (version 3.9.1) (Figure 2). A total of 85 components of PRA were obtained from the TCMSP database. After screening, 13 active ingredients were finally selected, and the targets of 13 active components were predicted by the Swiss Target Prediction. We found 116 potential drug targets for 8 active components. The best 19 targets, PGR, AR, CYP19A1, ESR1, ESR2, AGTR1, PTGS2, SHBG, NR3C1, CHRM2, GABRA2, PTPN11, PTGS1, PTPN1, NOS2, AKR1B10, PLA2G1B, SRC, and KDR, were discovered to have a greater degree in this process, emphasizing their prominence in the network (degree ≥ 5) (Table 3).

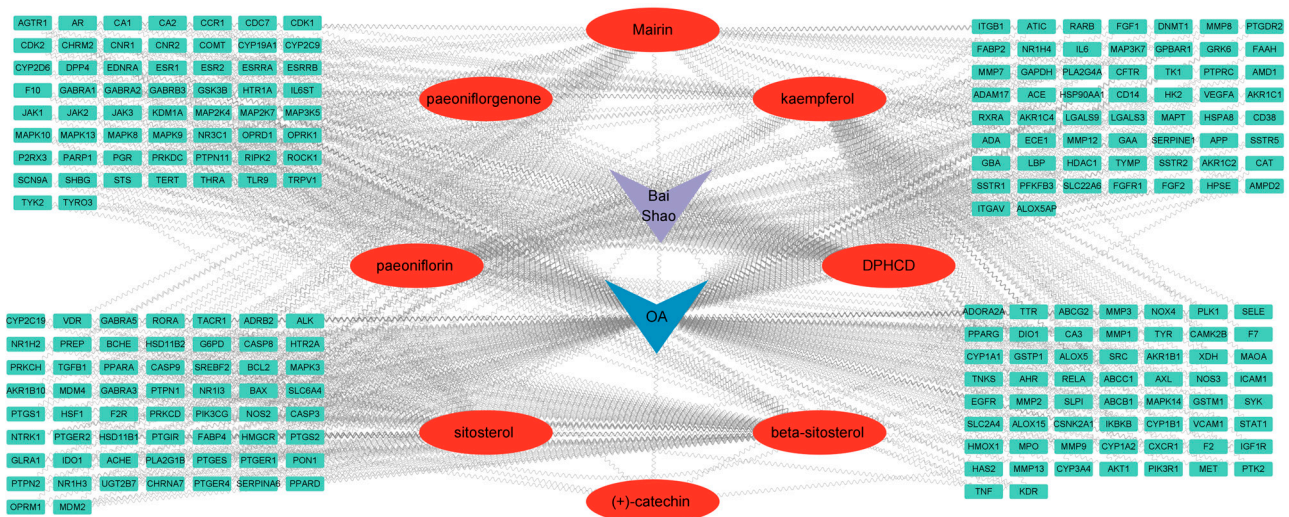


Figure 2. The PRA–OA–potential target gene network. The gray connecting lines indicate that each node is interconnected.

Table 3. Top 19 high-degree genes in the network.

NO	Target	Symbol	Betweenness Centrality	Closeness Centrality	Degree
1	Progesterone receptor	PGR	0.000649864	0.503131524	6
2	Androgen Receptor	AR	0.000649864	0.503131524	6
3	Cytochrome P450 19A1	CYP19A1	0.000649864	0.503131524	6
4	Estrogen receptor alpha	ESR1	0.002190625	0.503131524	6
5	Estrogen receptor beta	ESR2	0.000649864	0.503131524	6
6	Type-1 angiotensin II receptor (by homology)	AGTR1	0.000766102	0.503131524	6
7	Prostaglandin G/H synthase 2	PTGS2	0.001790972	0.501039501	6
8	Testis-specific androgen-binding protein	SHBG	0.000434223	0.501039501	5
9	Glucocorticoid receptor	NR3C1	0.000434223	0.501039501	5
10	Muscarinic acetylcholine receptor M2	CHRM2	0.00046555	0.501039501	5
11	Gamma-aminobutyric-acid receptor alpha-2 subunit	GABRA2	0.000461864	0.501039501	5
12	Protein-tyrosine phosphatase 2C	PTPN11	0.000434223	0.501039501	5
13	Prostaglandin G/H synthase 1	PTGS1	0.001790972	0.501039501	5
14	Protein-tyrosine phosphatase 1B	PTPN1	0.000519994	0.501039501	5
15	Nitric oxide synthase, inducible (by homology)	NOS2	0.000414611	0.501039501	5
16	Aldo-keto reductase family 1 member B10	AKR1B10	0.000414611	0.501039501	5
17	Phospholipase A2 group 1B	PLA2G1B	0.000414611	0.501039501	5
18	Tyrosine-protein kinase SRC	SRC	0.000542448	0.501039501	5
19	Vascular endothelial growth factor receptor 2	KDR	0.000542448	0.501039501	5

7.4. GO enrichment and KEGG Pathway Analysis

The entrezIDs of the 232 target genes are presented in Table 2. Examinations of these genes’ functional enrichment were performed to dig into any prospective physiological functions in the therapy of OA. According to the results, they were enriched with 2301 GO-BP terms, 152 GO-CC terms, and 289 GO-MF terms from the Metascape database ($p < 0.05$). A total of 20 significantly enriched gene physiological activity catalogs were chosen to generate a histogram for subsequent investigation (Figure 3A, Supplementary Figure S1). Our BP results (Figure 3B) indicated that the function of PRA active ingredients in OA is mainly concentrated upon hormone response, regulation of defense responses, cellular responses to lipids, responses to the molecule of bacterial origin, responses to inorganic components, response to extracellular stimulus, positive regulation of responses to external stimuli, regulation of MAPK cascades, protein phosphorylation, regulation of systemic processes, response to decreased oxygen levels, positive regulation of cell migration, response to a steroid hormone, response to wounding, positive regulation of cell death, circulatory system process, regulation of hormone levels, response to xenobiotic stimulus,

eicosane metabolic process, and rhythmic process. The MF items mainly contained protein serine/threonine/tyrosine kinase activity, nuclear receptor activity, oxidoreductase activity, protein tyrosine kinase activity, protein homodimerization activity, kinase binding, peptide binding, phosphatase binding, protein domain specific binding, carboxylic acid binding, MAP kinase activity, serine hydrolase activity, prostaglandin receptor activity, ligand-gated anion channel activity, cytokine receptor binding, non-membrane spanning protein tyrosine kinase activity, bile acid binding, heat shock protein binding, integrin binding, and virus receptor activity (Figure 3C). The CC items mainly included the membrane raft, receptor complex, side of membrane, dendrite, leading-edge membrane, vesicle lumen, neuron projection membrane, extracellular matrix, perinuclear region of cytoplasm, transcription regulator complex, nuclear envelope, lytic vacuole, endocytic vesicle, cytoplasmic side of the membrane, dendritic spine, outer organelle membrane, apical part of cell, endoplasmic reticulum lumen, and glutamatergic synapse (Figure 3D). These results suggest that PRA is associated with the therapy of OA through multiple gene biological functions, which will further clarify that PRA is beneficial against diseases, including OA.

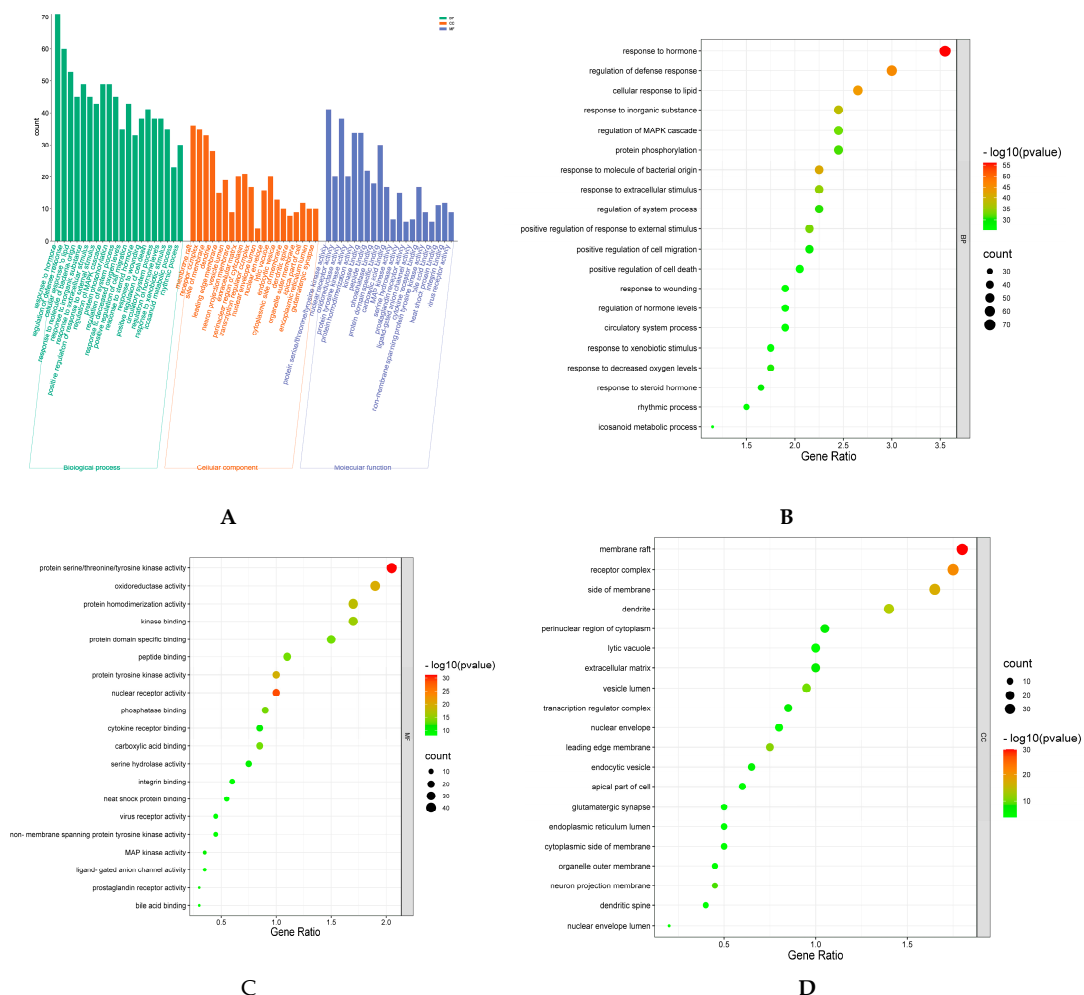


Figure 3. Functional enrichment analysis of the top 20 key gene ontology (GO) of PRA in the treatment of OA. (A) GO function analysis, including biological process (BP), cellular component (CC), and molecular function (MF). In the histogram, the common axis represents the degree of enrichment; (B) Bubble plot of Biological Processes (BP); (C) Bubble plot of Molecular Functions (MF); (D) Bubble plot of Cellular Components (CC). The top 20 key enriched GO terms are illustrated as bubble plots. GO terms with amended p -value < 0.01 were believed to be importantly enriched. X-axis, gene ratio (the ratio of targets in the background terms. bubble size, number of genes enriched. bubble color, p -value).

To further acquire a profound understanding of the mechanism of action of PRA in the treatment of OA, 209 signaling pathways were discovered by KEGG pathway enrichment analysis ($p < 0.05$) (Figure 4A,B). Scatterplots (Figure 4A) and histograms (Supplementary Figure S2) are listed using the top 20 crucial signaling pathways. As shown in Figure 4A, various signaling pathways are deeply connected with OA, including pathways in cancer, the VEGF signaling pathway, the chemokine signaling pathway, the NF-kappa B signaling pathway, and regulating pluripotency of stem cells signaling pathways (Figure 4B). According to the KEGG analysis results, 20 significant therapeutic pathways were contained in the targets shown in Table 4. Furthermore, the KEGG mapper was used to color targets red in the significant NF-kappa B signaling pathway, as shown in Figure 5.

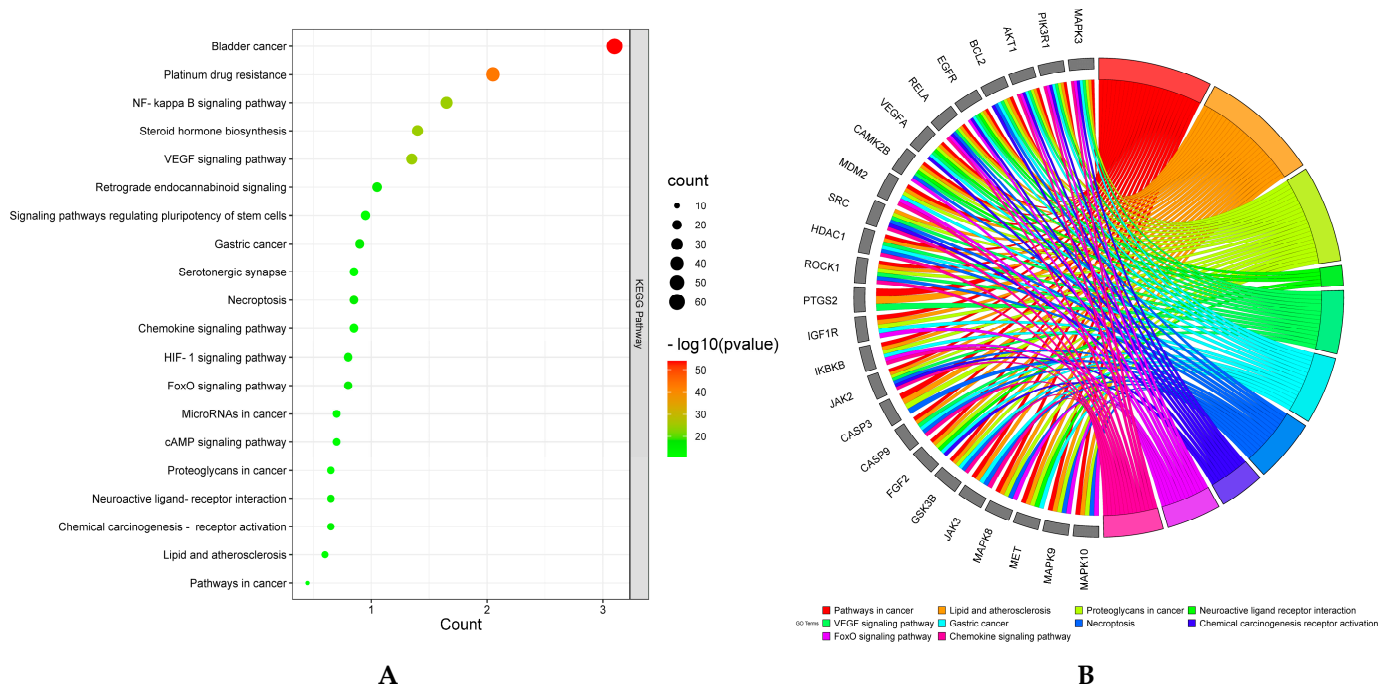


Figure 4. Kyoto Encyclopedia of Genes and Genomes (KEGG) pathway enrichment analyses of PRA for OA. (A) The first 20 significantly enriched KEGG pathways are shown as bubble points. KEGG pathways with regulated p -value < 0.01 were greatly enriched. The x -axis, count. Bubble size, massive genes enriched. Bubble color, p -value; (B) Enrichment analysis of KEGG pathway related to the therapy of OA with PRA.

Table 4. KEGG pathway analysis results.

Pathway Name	Symbol
Pathways in cancer	AGTR1, AKT1, ALK, AR, BAX, BCL2, CAMK2B, CASP3, CASP8, CASP9, CDK2, EDNRA, EGFR, ESR1, ESR2, F2, F2R, FGF1, FGF2, FGFR1, GSK3B, GSTM1, GSTP1, HDAC1, HMOX1, HSP90AA1, IGF1R, IKBKB, IL6, IL6ST, ITGAV, ITGB1, JAK1, JAK2, JAK3, MDM2, MET, MMP1, MMP2, MMP9, NOS2, NTRK1, PIK3R1, PPAR, PARG, MAPK3, MAPK8, MAPK9, MAPK10, PTGER1, PTGER2, PTGER4, PTGS2, PTK2, RARB, RELA, ROCK1, RXRA, STAT1, TERT, TGFB1, VEGFA
Lipid and atherosclerosis	AKT1, BAX, BCL2, CAMK2B, CASP3, CASP8, CASP9, CD14, MAPK14, CYP1A1, CYP2C9, GSK3B, HSPA8, HSP90AA1, ICAM1, IKBKB, IL6, JAK2, LBP, MAP3K5, MMP1, MMP3, MMP9, NOS3, PIK3R1, PPAR, MAPK3, MAPK8, MAPK9, MAPK10, MAPK13, MAP2K7, PTK2, RELA, RXRA, SELE, MAP2K4, SRC, MAP3K7, TNF, VCAM1, GSTM1, GSTP1, HMOX1, ITGAV, KDR, MMP2, VEGFA, AGTR1, SERPINE1, PRKCD, STAT1, TGFB1, NOX4, CCR1, FGF2, IL6ST, JAK1, PIK3CG, PTGS2, SYK, TYK2, CDK2, JAK3, AHR, CAT, AKR1C4, CYP1A2, CYP1B1, AKR1C1, AKR1C2, EGFR, MET, PTPN1, PTPN11, ALOX5, ITGB1, NOS2, VDR, RIPK2, TLR9, HDAC1, MDM2, CSNK2A1, MMP13, CYP2D6, ESR1, ESR2, IGF1R, RORA, NTRK1, ACE, PPARA, HK2, ROCK1, GAPDH, PTPRC, NR1H3, F2, ADAM17, F2R, SLC2A4, NR1H2, PARP1, G6PD, ALOX5AP, PLA2G4A, CXCR1, HTR2A, PRKCH, PTGER2, PTGER4, TRPV1, ABCG1, OPRD1, ALK, CDK1, APP, CHRNA7, MAPT, SSTR1, SSTR2, SSTR5, MMP7, TERT, COMT, MAOA
Chemical carcinogenesis—receptor activation	ADRB2, AHR, AKT1, AR, BCL2, CHRNA7, CYP1A1, CYP1A2, CYP1B1, CYP3A4, EGFR, ESR1, ESR2, FGF2, GSTM1, HSP90AA1, JAK2, PGR, PIK3R1, PPARA, MAPK3, RELA, RXRA, SRC, UGT2B7, VDR, VEGFA, NR1I3, HSPA8, MMP2, MMP9, NOS3, OPRM1, PRKCD

Table 4. Cont.

Pathway Name	Symbol
Neuroactive ligand receptor interaction	ADORA2A, ADRB2, AGTR1, CHRM2, CHRNA7, CNR1, CNR2, EDNRA, F2, F2R, GABRA1, GABRA2, GABRA3, GABRA5, GABRB3, GLRA1, NR3C1, HTR1A, HTR2A, OPRD1, OPRK1, OPRM1, P2RX3, PTGER1, PTGER2, PTGER4, PTGIR, SSTR1, SSTR2, SSTR5, TACR1, THRA, TRPV1, CAMK2B, CD38, EGFR, FGF1, FGF2, FGFR1, KDR, MET, NOS2, NOS3, NTRK1, VEGFA
Proteoglycans in cancer	AKT1, CAMK2B, CASP3, MAPK14, EGFR, ESR1, FGF2, FGFR1, IGF1R, ITGAV, ITGB1, KDR, MDM2, MET, MMP2, MMP9, PIK3R1, MAPK3, MAPK13, PTK2, PTPN11, ROCK1, SRC, TGFB1, TNF, VEGFA, HPSE, CD14, FGF1, HSPA8, IKBKB, MAPT, MAP3K5, NTRK1, PLA2G4A, MAPK8, MAPK9, MAPK10, MAP2K7, RELA, MAP2K4, MAP3K7, AXL, BAX, BCL2, GSK3B, IL6, JAK1, JAK2, PLA2G1B, ADORA2A, CNR1, F2R
HIF-1 signaling pathway	AKT1, BCL2, CAMK2B, EGFR, GAPDH, HK2, HMOX1, IGF1R, IL6, NOS2, NOS3, SERPINE1, PFKFB3, PIK3R1, MAPK3, RELA, VEGFA
FoxO signaling pathway	AKT1, CAT, CDK2, MAPK14, EGFR, IGF1R, IKBKB, IL6, MDM2, PIK3R1, PLK1, MAPK3, MAPK8, MAPK9, MAPK10, MAPK13, SLC2A4, TGFB1, CDK1, HSP90AA1, PGR, SERPINE1, RELA, AR, CAMK2B
cAMP signaling pathway	ADORA2A, ADRB2, AKT1, CAMK2B, CFTR, CHRM2, EDNRA, F2R, HTR1A, PIK3R1, PPARA, MAPK3, MAPK8, MAPK9, MAPK10, PTGER2, RELA, ROCK1, SSTR1, SSTR2, SSTR5
Serotonergic synapse	ALOX5, ALOX15, APP, CASP3, CYP2C19, CYP2C9, CYP2D6, GABRB3, HTR1A, HTR2A, MAOA, PLA2G4A, MAPK3, PTGS1, PTGS2, SLC6A4
VEGF signaling pathway	AKT1, CASP9, MAPK14, KDR, NOS3, PIK3R1, PLA2G4A, MAPK3, MAPK13, PTGS2, PTK2, SRC, VEGFA, F2, F2R, ITGB1, PIK3CG, PTGIR, PTGS1, ROCK1, SYK, AGTR1, EGFR, CXCR1, PTPN11, ACHE, BCL2, CAMK2B, CHRM2, CHRNA7, JAK2, HDAC1, MPO, RELA, MAP3K7, CD38, ADRB2, EDNRA, OPRD1, NOS2, SERPINE1
Steroid hormone biosynthesis	STS, AKR1C4, COMT, CYP11A1, CYP11B1, CYP17A1, CYP19A1, AKR1C1, AKR1C2, HSD11B1, HSD11B2, UGT2B7, CYP2C19, CYP2C9, GSTM1, GSTP1, PTGS2, CYP2D6, MAOA, CAT, IDO1
Necroptosis	PARP1, ALOX15, BAX, BCL2, CAMK2B, CASP8, HSP90AA1, JAK1, JAK2, JAK3, PLA2G4A, MAPK8, MAPK9, MAPK10, STAT1, TNF, TYK2, CASP3, CASP9, CSNK2A1, GSK3B, MMP7, PPARD, MAP3K7, CFTR, ITGB1, MAP3K5, MAP2K7, ROCK1, SRC, ADORA2A, MAOA, MAPT, HSPA8, RELA, HDAC1, PPARG
Gastric cancer	AKT1, BAX, BCL2, CDK2, EGFR, FGF1, FGF2, GSK3B, MET, ABCB1, PIK3R1, MAPK3, RARB, RXRA, TERT, TGFB1, FGFR1, IGF1R, MDM2, ALK, CASP9, JAK3, ESR1, ESR2, PGR, HDAC1, IKBKB, PTPN11, RELA, GSTM1, GSTP1, HMOX1, G6PD, HK2, NTRK1, CD14, MPO, PPARD, CAMK2B, VEGFA, SYK, PLA2G4A, PRKCD, PTPRS2, TNF, HSD11B2
Chemokine signaling pathway	AKT1, CCR1, GRK6, GSK3B, IKBKB, CXCR1, JAK2, JAK3, PIK3CG, PIK3R1, PRKCD, MAPK3, PTK2, RELA, ROCK1, SRC, STAT1, CASP9, DIO1, ESR1, HDAC1, ITGAV, MDM2, RXRA, THRA
Platinum drug resistance	AKT1, BAX, BCL2, CASP3, CASP8, CASP9, GSTM1, GSTP1, MDM2, MAP3K5, PIK3R1, MAPK3, CDK1, CDK2, HDAC1, IL6ST, JAK1, JAK3, RELA, SRC, SYK, MDM4, SERPINE1
NF-kappa B signaling pathway	PARP1, BCL2, CD14, CSNK2A1, ICAM1, IKBKB, LBP, PTGS2, RELA, SYK, MAP3K7, TNF, VCAM1
MicroRNAs in cancer	BCL2, CASP3, CYP11B1, DNMT1, EGFR, HDAC1, HMOX1, IKBKB, MDM2, MDM4, MET, MMP9, ABCB1, ABCB1, PIK3R1, MAPK3, PTGS2, ROCK1, VEGFA
Signaling pathways regulating pluripotency of stem cells	AKT1, MAPK14, ESRB, FGF2, FGFR1, GSK3B, IGF1R, IL6ST, JAK1, JAK2, JAK3, PIK3R1, MAPK3, MAPK13, BCL2, EGFR, IL6, PTPN2, PTPN11, STAT1, TYK2
Retrograde endocannabinoid signaling	CNR1, MAPK14, FAAH, GABRA1, GABRA2, GABRA3, GABRA5, GABRB3, MAPK3, MAPK8, MAPK9, MAPK10, MAPK13, PTGS2, CHRNA7, HTR1A, P2RX3, SCN9A, GRK6, OPRM1, SRC
Bladder cancer	TYMP, EGFR, MDM2, MMP1, MMP2, MMP9, MAPK3, SRC, VEGFA, CSNK2A1, FGFR1, IGF1R, MET, PTPN1, MAP3K7, CDK1, HTR2A, GRK6, HSPA8, CXCR1

7.5. Analysis of Molecular Docking Results

Molecular docking was executed to verify the binding ability of AKT1, CASP3, GAPDH, ICAM1, IL-6, MAPK3, MMP9, PTGS2, TNF, and VEGFA, with Mairin, be-tasitosterol, sitosterol, kaempferol, (+)-catechin, paeoniflorone, DPHCD, paeoniflorin, in line with network analysis and preliminary research. When the binding energy is small, it indicates that the binding degree of the ligand to the target protein is high. The molecular binding energy ranges from -6 to -10.3 kcal/mol, indicating that the binding energy results have good binding activity (Figure 6). The results in Figure 6 show that the representative components of PRA have a better binding activity to the core target, which, to a certain extent, verifies the reliability of the preliminary results of network pharmacology. Figure 7A–F shows the 3D binding map and hydrogen bond map of the optimal combination of 3 core components and their optimal target proteins in the active components of PRA. As shown in Figure 7A, kaempferol could form a structure of two hydrogen bonds with MET-522 and LEU-535 in PTGS2, and their bond lengths were 2.5 and 2.4. As shown in Figure 7B, (+)-catechin could form a hydrogen bond with GLN-461 and GLY-45 in PTGS2, and their bond lengths were 2.8 and 2.0. As shown in Figure 7C, DPHPD could form 1 hydrogen bond with GLN-372 in PTGS2 with a bond length of 2.4. As shown in Figure 7D, kaempferol could form 1, 2, and 3 hydrogen bonds with LEU-188, GLN-227, and ALA-189

in MMP9, with bond lengths of 2.7, 2.4, 2.1, 2.2, 2.5, and 3.5, respectively. As shown in Figure 7E, (+)-catechin could form a hydrogen bond with LEU-243 and LEU-188 in MMP9, respectively, and the bond lengths are 2.5, 2.2, and 2.9, respectively. As shown in Figure 7F, DPHCD could form 1 hydrogen bond with ALA-199 in MMP 9 with a bond length of 2.5.

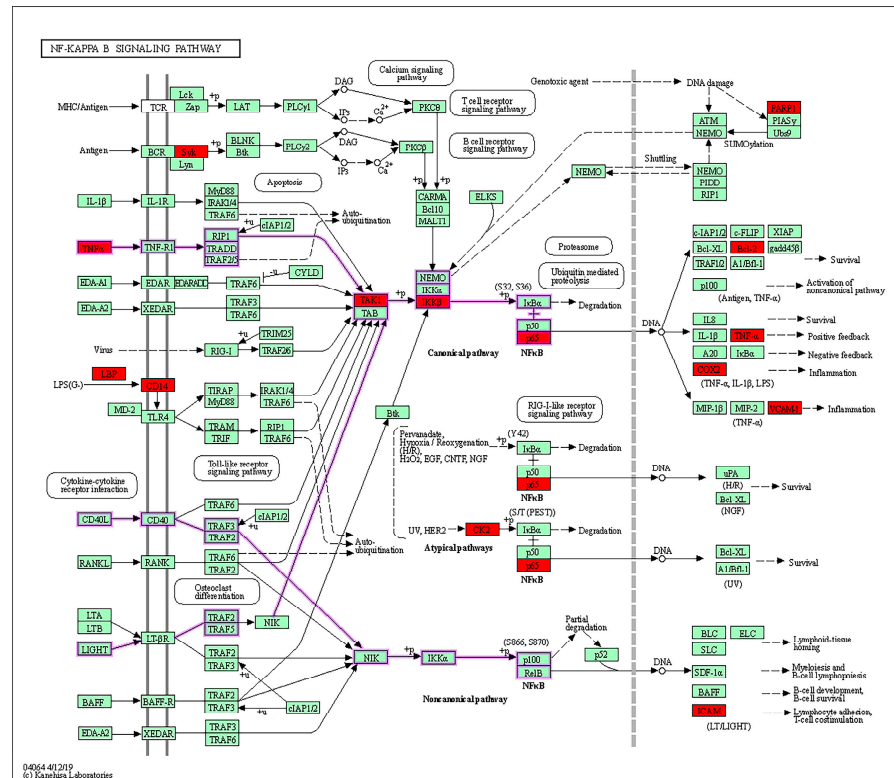


Figure 5. The NF-kappa B signaling pathway of potential target genes relationship between PRA and OA. The purple arrows mainly indicate the upstream–downstream relationship between genes. The red is a PRA target gene in the network.

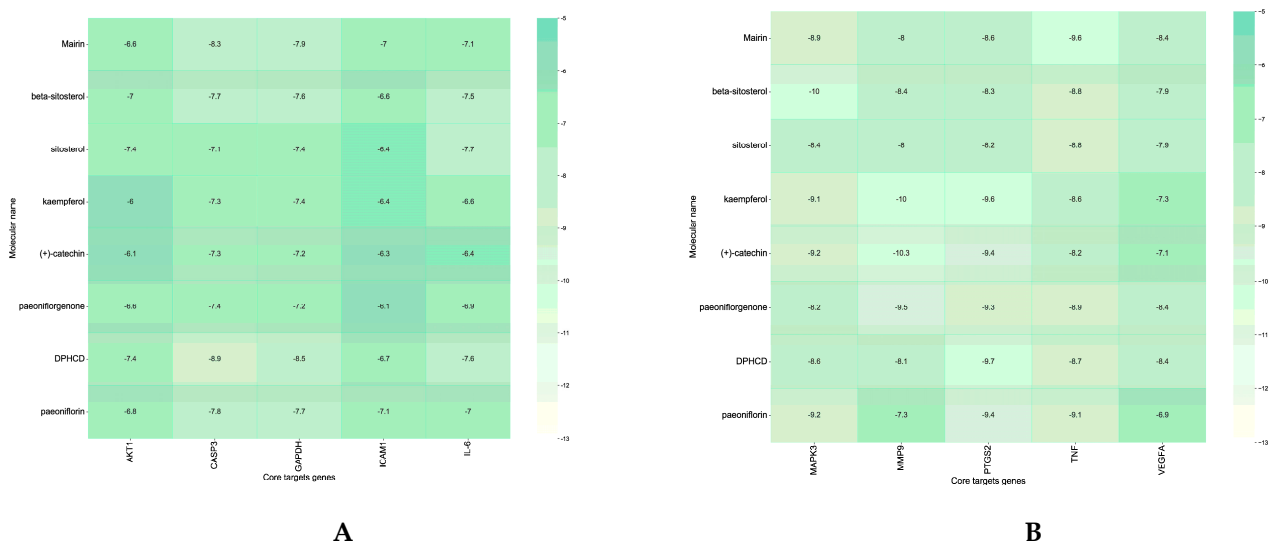


Figure 6. Heat map of binding energies 8 active components and 10 core genes in PRA (A,B).

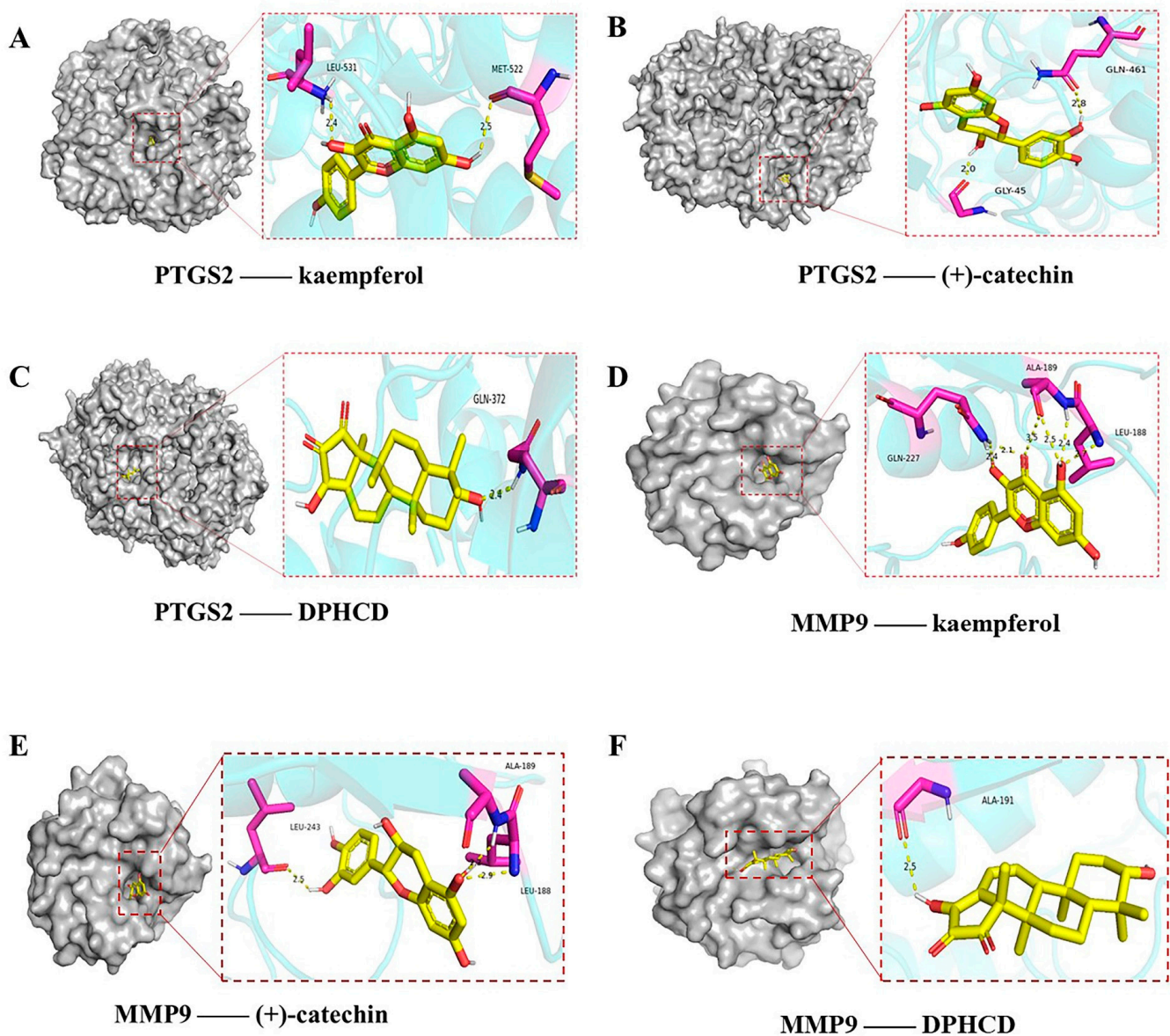


Figure 7. The 6 best docking results of 3 compounds and 2 core targets. The docking between kaempferol and PTGS2 (A), (+)-catechin and PTGS2 (B), DPHCD and PTGS2 (C), kaempferol and MMP9 (D), (+)-catechin and MMP9 (E), DPHCD and MMP9 (F). The yellow structural formula represents the active ingredient. The protein targets bound to the active ingredient are shown as purple rods, and the binding sites are linked by yellow hydrogen bonds.

In conclusion, there is an interaction between core genes with different bonds and key active ingredients. Our results show that the three key active ingredients in PRA can have a stronger binding force to PTGS2 and MMP9 to produce a therapeutic effect on OA.

8. Discussion

Osteoarthritis (OA) is a common degenerative joint disease that primarily affects 10% of men and 18% of women over 60 years of age; major signs include arthritis, synovial inflammation, joint edge, and underlying subchondral bone lesions, which poses a serious health threat and decreases the quality of life [56,57]. Currently, the representative drugs for the treatment of OA include selective COX-2 enzyme inhibitors, non-steroidal anti-inflammatory drugs (NSAIDs), glucocorticoids, viscosupplements, and other conventional medicines [58]. However, the choice of medical therapy for OA is still debatable because most of the medications used today are primarily intended to address patients' pain,

inflammatory symptoms, and other uncomfortable symptoms rather than prevent or treat the disease and have high toxicity and poor efficacy.

It is worth mentioning that Traditional Chinese Medicine (TCM) functions have been progressively implemented in the prevention and treatment of OA due to their significant tonifying of the liver and kidney, comforting of tendons, activation of blood circulation, dredging of collateral and alleviating pain, long-term efficacy, few adverse effects, and has been identified by the majority of patients [59]. The mechanism of OA is associated with numerous variables, including pro-inflammatory and anti-inflammatory cytokines and cytokine/receptor signaling pathways [60,61]. Radix *Paeoniae Alba* has a major advantage in treating OA as a significant blood-activating, pain-relieving medication, but further research into its precise molecular mechanism is needed [11]. In the present study, 13 candidate ingredients of PRA were found to play significant roles in the treatment of OA and to be associated with various proteins and signaling pathways, suggesting that these candidate constituents have a potential research value.

The 13 representative ingredients from PRA collection results were widely investigated and verified, demonstrating that they have positive effects on immunity and inflammation. However, there have been a few investigations on OA treatment by PRA, and most of them tended to concentrate on the isolated components from PRA, which required systematic insights and depth [62]. Unfortunately, massive constituents of Chinese herbal medicine have specific curative effects in experiments but are less than satisfactory in clinical applications [63].

Network pharmacology, which is based on the theoretical advancement of multi-directional pharmacology, systems biology, and omics, is a booming research approach for the design and development of new drugs with the development of systems biology technology. The multi-component, multi-target, and systematic regulation notions are embodied in the holistic perspective of TCM and the syndrome differentiation and therapy concept, which shares massive parallels with the network pharmacology research idea [64]. Based on many experimental data and clinical trial results, network pharmacology could be used to analyze the potential mechanism of clinical treatment and precaution of diseases, particularly appropriate for the characteristics of intricate components and multiple targets and mechanisms of TCM. Therefore, this study aims to unveil the anti-OA mechanism of PRA. In addition, the molecular docking pattern between the compound and the target indicated an excellent combination, further verified by the intrinsic relationship between PRA and OA.

According to the PPI network map of PRA therapy for OA, it was determined that paeoniflorone, DPHCD, beta-sitosterol, kaempferol, (+)-catechin, paeoniflorin, sitosterol, and Mairin were the most central potential therapeutic components of PRA anti-OA. Kaempferol has been recognized as an effective agent for alleviating the clinical symptoms of OA. Previous studies found that kaempferol inhibits interleukin-1 β and, thus, inhibits cartilage damage by RANKL and MAOKs [65]. Zhuang and his colleague's research revealed that kaempferol alleviates the interleukin-1 β -induced inflammation in rat OA chondrocytes via suppression of NF- κ B had significant anti-inflammatory and anti-arthritis effects [66]. In addition, kaempferol activates the PI3K/AKT/mTOR signaling pathway by downregulating miR-146 and inhibiting Decurion expression [67]. Cheng B C et al. pointed out that paeoniflorin can protect cartilage by targeting (IL)-1 β in the NF- κ B pathway [49]. However, no primary research on beta-sitosterol in the treatment of OA has been reported so far, and further research is worthy of following-up. Studies of other components have shown evidence that (+)-catechin normalizes the gene expression levels of inflammatory cytokines such as COX-2, TNF- α , IL-1 β , IL-6, and NF- κ B [68]. In summary, the 8 active components of PRA have different therapeutic effects on OA, involving a diverse range of cytokines and signaling pathways and warrant deep exploration.

We applied a PPI network (Figure 2); many of the 8 compounds can regulate many target genes in OA in PRA. These genes contain but are not limited to NR3C, CHRM2, GABRA2, PTPN11, PTGS1, PTPN1, and NOS2. This point completely reflected the charac-

teristics of multi-target and multi-component Traditional Chinese Medicine. Additionally, the PPI results further show that the 232 target proteins are related and interact rather than exist independently [69]. As shown in Table 2, PGR, AR, CYP19A1, ESR1, ESR2, AGTR1, and PTGS2 were the important target genes in the PPI network.

We used GO and KEGG enrichment analysis to identify the 232 possible targets directly connected to the formation and progression of OA to anticipate the biological processes and signaling pathways that may underlie the therapeutic impact of PRA in OA. The 20 significantly enriched KEGG keywords that mainly were connected to pathways in cancer, VEGF signaling pathway, chemokine signaling pathway, NF- κ B signaling pathway, FoxO signaling pathway, and regulating pluripotency of stem cells signaling pathways are depicted in Figure 4. Inflammation has a vital and close relationship with the pathogenesis of OA. The NF- κ B pathway is a classic pathway highly related to OA. Some studies have revealed that several mouse models of OA in the NF- κ B pathway were better-characterized signaling pathways loading in the animal model of OA [70,71]. The study showed that downregulating NF- κ B signaling can prevent cartilage degeneration partially [72]. Inhibition of NF- κ B Activity and chondrocyte pyroptosis may ameliorate cartilage degeneration and development in OA [73,74]. The HIF-1 signaling pathway contributes to many autoimmune diseases containing OA [75,76]. HIF-1 plays a fundamental role in chondrocyte survival and maintains the homeostatic conditions of articular cartilage, which regulate both autophagy and apoptosis [77]. Previous research has shown that activated or inhibitors of the HIF-1 signaling pathway can cure OA [78,79]. The study of the HIF-1 signaling pathway helps to reveal the pathogenesis of OA and reduces abnormal inflammation, providing potential targets. Angiogenesis occupies a pivotal position in OA. Vascular endothelial growth factor (VEGF) is a pro-inflammatory factor that directly affects vascular endothelial cells and early neovascularization, ultimately leading to joint inflammation in OA. In recent years, cumulative evidence has shown that angiogenesis plays a substantial part in synovitis, osteochondral channel formation, joint marginal osteophyte formation and joint pain in OA and is one of the crucial factors in the formation and aggravation of OA [80,81]. Recent studies have reported that increasing VEGF expression and promoting EPC angiogenesis in OA synovial fibroblasts (OASFs) by inhibiting miR-485-5p synthesis via PI3K and Akt signaling could be used to treat OA [82].

Additionally, inhibition of VEGF overexpression contributes to the recovery from OA [83]. Furthermore, we also found other pathways, such as pathways in cancer, lipid and atherosclerosis, chemical carcinogenesis–receptor activation, neuroactive ligand–receptor interaction, proteoglycans in cancer, cAMP signaling pathway, serotonergic synapse, and steroid hormone biosynthesis, indicating that PRA has potential applications in tumors, atherosclerosis, and other diseases. Based on the aforementioned multiple pathways, it is speculated that PRA cures OA by the inflammatory response, immune regulation, and other processes. In addition, to further explore the potential molecular mechanism of PRA in the treatment of OA, we screened 8 active compounds as ligands and conducted molecular docking studies on 10 targets closely related to OA. The results showed that the 2 potential target genes had a better binding to the 3 active compounds.

Traditional Chinese Medicine (TCM) stands as one of the crown jewels of Chinese culture, boasting a rich history of use across East Asia and Southeast Asia, and has been extensively employed since the dawn of ancient civilizations. With the rapid development of bioinformatics, systems biology, and multi-pharmacology, network-based drug discovery is considered a promising and cost-effective method for drug development. At present, a large number of pertinent databases and tools offer vital support for the field of network pharmacology in TCM. Databases frequently employed in the network pharmacology of TCM include TCMSp [84], drug information databases [85], PubChem [86], target interaction databases [87], and gene–disease association databases [88], which provide an understanding of the effects of herbs on diseases. The network pharmacology algorithm is a frequently employed network clustering technique that commences with a random node (drug, target, or disease), computes the similarity between that node and its neigh-

boring nodes, and constructs a “drug–target–disease” network. In addition, the tools and databases employed in the field of TCM network pharmacology are founded on constraints imposed on ranking functions. These constraints take into account the smoothness of the network and the utilization of prior information to prioritize disease genes and deduce the associations among protein complexes. In addition to data acquisition and analysis, visualization is a crucial component of network pharmacology, rendering the network more intuitive. Cytoscape is an open-source platform designed for visualizing molecular interaction networks and biological pathways, while integrating these networks with annotations, gene expression profiles, and other data on gene states. Currently, most databases include web services that can transfer data between databases, serving as a conversion platform. These services are presented to users as web services integrated with various databases or browser plugins, ensuring their reliability. Currently, TCM has documented over 10,000 herbs used in more than 100,000 formulas [89]. However, research in network pharmacology for TCM is nascent and requires further development. Additionally, as data from TCM and clinical research accumulate, and with the interaction of various analytical and experimental methods, researchers can gain more substantial and authentic insights.

9. Conclusions and Future Perspective

The single target/single molecule, side effects, drug resistance, and decreased effectiveness of current medications continue to limit their ability to prevent OA and its progression. This is true even with the advancements in modern therapeutics. From the perspective of drug development, network-based drug discovery is seen as a viable and cost-effective approach, especially considering the rapid advancements in system biology, bioinformatics, and polypharmacology. PRA also has a wide variety of biological traits and structural polymorphism, which provides opportunities to find different lead entities. In the present study, we investigated the effective active ingredients and molecular mechanisms of PRA in the treatment of OA by the network pharmacology approach. The most significant potential 8 active ingredients of PRA in OA treatment were screened out that involves 232 target genes correlated with OA, among which AKT1, CASP3, GAPDH, ICAM1, IL-6, MAPK3, MMP9, PTGS2, TNF, VEGFA are identified as core target genes. Paeoniflorone, DPHCD, beta-sitosterol, kaempferol, (+)-catechin, paeoniflorin, sitosterol, and Mairin were identified as the essential phytochemicals treating OA. The signaling pathways of PRA in the treatment of OA mainly contain the HIF-1 signaling pathway, FoxO signaling pathway, VEGF signaling pathway, Necroptosis, and NF- κ B signaling pathway. In addition, we verified the most positive effect on OA of the active components kaempferol, (+)-catechin, and DPHCD by molecular docking.

Despite the fact that PRA has demonstrated anti-inflammatory and pain-relieving properties for osteoarthritis in pre-clinical research, human study data is still lacking; therefore, conclusions cannot be made. Therefore, clinical trials are required to determine the best way to administer them to patients with osteoarthritis (OA) as well as the ideal dosage for pain and inflammation alleviation. Moreover, a lack of research calls for the quick development and application of innovative network approaches to challenge accepted theories about drug discovery and expand our understanding of action principles. Using network pharmacology with PRA can help open up new ways of addressing the limitations of the treatments that are now available to prevent OA.

10. Study Limitations

Although network pharmacology is a fast and effective method for predicting multiple drug targets in complex diseases, there are also some shortcomings; for example:

- (1) The ingredients in TCM are incredibly complex, and the ingredients that play a therapeutic role under the action of metabolic enzymes after absorption by the human body are not all the prototype ingredients of TCM; both OB and DL values of chemical ingredients are used to screen the chemical ingredients of active ingredients, so the tissue distribution of bioavailability of Chinese medicine cannot be quantified objectively.

- (2) Network pharmacology matches relevant information from public databases, but the existing databases lack a unified standard.
- (3) Obtaining disease targets by searching disease-related databases ignores the pathophysiological changes of diseases in the clinical development process and lacks objectivity.
- (4) The foundation of the therapeutic effect in Traditional Chinese Medicine does not necessarily lie in a single chemical compound but rather in the collective action of many chemical compounds. Consequently, research focused on the efficacy of chemical drugs targeting single pathways is not fully applicable to the study of the therapeutic effects of Traditional Chinese Medicine.
- (5) In this study, the number of components was not considered. However, the impact of both quantity and concentration on therapeutic efficacy cannot be disregarded. Only when a sufficient quantity of the drug reaches the target site can it effectively deliver its therapeutic effect.
- (6) In this study, the quantity of active ingredients in PRA was not taken into account, and the effect of the quantity of ingredients on the efficacy of the drug was overlooked.

In the present study, the interaction between the active ingredient of PRA and the biological function of the target is ignored, and the molecular binding between the active ingredient and the target of the non-intersection ingredient is seldom considered. In addition, PRA anti-OA has not been further validated by animals and cell models of corresponding OA.

Supplementary Materials: The following supporting information can be downloaded at <https://www.mdpi.com/article/10.3390/separations11060184/s1>: Supplementary Table S1. The 706 target genes of PRA active ingredients. Supplementary Figure S1. The top 20 remarkably enriched GO analysis for biological function of potential target genes of PRA anti-OA. (A) GO-BP terms; (B) GO-CC terms; (C) GO-MF terms; ($p < 0.05$). Supplementary Figure S2. The top 20 remarkably enriched KEGG analysis for signaling pathway of potential target genes of PRA anti-OA; ($p < 0.05$).

Author Contributions: B.W.: Investigation, Methods, Drawing, Writing the first draft, drawing graphic abstracts, scatter plots, histograms, and organizing data. Y.Z. and C.B.: Helped with topic selection and reviewed and finalized the paper. All authors have read and agreed to the published version of the manuscript.

Funding: This work was supported by grants from the National Natural Science Foundation of China (No. 81860755).

Data Availability Statement: The data are available for reproduction of results on request from the corresponding author.

Conflicts of Interest: The authors declare no conflicts of interest.

References

1. McAllister, M.; Chemaly, M.; Eakin, A.J.; Gibson, D.S.; McGilligan, V.E. NLRP3 as a potentially novel biomarker for the management of osteoarthritis. *Osteoarthr. Cartil.* **2018**, *26*, 612–619. [[CrossRef](#)]
2. Nelson, A.E.; Schwartz, T.A.; Alvarez, C.; Golightly, Y.M. The prevalence of hand osteoarthritis: Comment on the article by Eaton et al. *Arthritis Rheumatol.* **2022**, *74*, 1861–1862. [[CrossRef](#)]
3. Sok, D.; Raval, S.; McKinney, J.; Drissi, H.; Mason, A.; Mautner, K.; Kaiser, J.M.; Willett, N.J. NSAIDs Reduce Therapeutic Efficacy of Mesenchymal Stromal Cell Therapy in a Rodent Model of Posttraumatic Osteoarthritis. *Am. J. Sports Med.* **2022**, *50*, 1389–1398. [[CrossRef](#)]
4. Zhang, T.; Chen, S.; Dou, H.; Liu, Q.; Shu, G.; Lin, J.; Zhang, W.; Peng, G.; Zhong, Z.; Fu, H. Novel glucosamine-loaded thermosensitive hydrogels based on poloxamers for osteoarthritis therapy by intra-articular injection. *Mater. Sci. Eng. C Mater. Biol. Appl.* **2021**, *118*, 111352. [[CrossRef](#)]
5. Knoop, J.; Dekker, J.; van Dongen, J.M.; van der Leeden, M.; de Rooij, M.; Peter, W.F.; de Joode, W.; van Bodegom-Vos, L.; Lopuhaä, N.; Bennell, K.L.; et al. Stratified exercise therapy does not improve outcomes compared with usual exercise therapy in people with knee osteoarthritis (OCTOPuS study): A cluster randomised trial. *J. Physiother.* **2022**, *68*, 182–190. [[CrossRef](#)]
6. Padilla-Martinez, J.P.; Lewis, W.; Ortega-Martinez, A.; Franco, W. Intrinsic fluorescence and mechanical testing of articular cartilage in human patients with osteoarthritis. *J. Biophotonics* **2018**, *11*, e201600269. [[CrossRef](#)]

7. Talaie, R.; Torkian, P.; Clayton, A.; Wallace, S.; Cheung, H.; Chalian, M.; Golzarian, J. Emerging Targets for the Treatment of Osteoarthritis: New Investigational Methods to Identify Neo-Vessels as Possible Targets for Embolization. *Diagnostics* **2022**, *12*, 1403. [[CrossRef](#)]
8. Ma, L.; Zheng, X.; Lin, R.; Sun, A.R.; Song, J.; Ye, Z.; Liang, D.; Zhang, M.; Tian, J.; Zhou, X.; et al. Knee Osteoarthritis Therapy: Recent Advances in Intra-Articular Drug Delivery Systems. *Drug Des. Devel Ther.* **2022**, *16*, 1311–1347. [[CrossRef](#)]
9. Rai, V.; Khatoon, S.; Bisht, S.; Mehrotra, S. Effect of cadmium on growth, ultramorphology of leaf and secondary metabolites of *Phyllanthus amarus* Schum. and Thonn. *Chemosphere* **2005**, *61*, 1644–1650. [[CrossRef](#)] [[PubMed](#)]
10. Zhao, Y.; Zhang, Y.; Kong, H.; Zhang, M.; Cheng, J.; Wu, J.; Qu, H.; Zhao, Y. Carbon Dots from *Paeoniae Radix Alba* Carbonisata: Hepatoprotective Effect. *Int. J. Nanomed.* **2020**, *15*, 9049–9059. [[CrossRef](#)] [[PubMed](#)]
11. Tan, Y.-Q.; Chen, H.-W.; Li, J.; Wu, Q.-J. Efficacy, chemical constituents, and pharmacological actions of *Radix Paeoniae Rubra* and *Radix Paeoniae Alba*. *Front. Pharmacol.* **2020**, *11*, 1054. [[CrossRef](#)] [[PubMed](#)]
12. Liu, L.; Yuan, Y.; Tao, J. Flavonoid-Rich Extract of *Paeonia lactiflora* Petals Alleviate d-Galactose-Induced Oxidative Stress and Restore Gut Microbiota in ICR Mice. *Antioxidants* **2021**, *10*, 1889. [[CrossRef](#)] [[PubMed](#)]
13. Zheng, X.; Yin, M.; Chu, S.; Yang, M.; Yang, Z.; Zhu, Y.; Huang, L.; Peng, H. Comparative Elucidation of Age, Diameter, and “Pockmarks” in Roots of *Paeonia lactiflora* Pall. (Shaoyao) by Qualitative and Quantitative Methods. *Front. Plant Sci.* **2021**, *12*, 802196. [[CrossRef](#)] [[PubMed](#)]
14. Zhou, C.; Zhang, Y.; Sheng, Y.; Zhao, D.; Lv, S.; Hu, Y.; Tao, J. Herbaceous peony (*Paeonia lactiflora* Pall.) as an alternative source of oleanolic and ursolic acids. *Int. J. Mol. Sci.* **2011**, *12*, 655–667. [[CrossRef](#)] [[PubMed](#)]
15. Yan, B.F.; Chen, X.; Chen, Y.F.; Liu, S.J.; Xu, C.X.; Chen, L.; Wang, W.B.; Wen, T.T.; Zheng, X.; Liu, J. Aqueous extract of *Paeoniae Radix Alba* (*Paeonia lactiflora* Pall.) ameliorates DSS-induced colitis in mice by tuning the intestinal physical barrier, immune responses, and microbiota. *J. Ethnopharmacol.* **2022**, *294*, 115365. [[CrossRef](#)] [[PubMed](#)]
16. Li, X.; Wang, W.; Su, Y.; Yue, Z.; Bao, J. Inhibitory effect of an aqueous extract of *Radix Paeoniae Alba* on calcium oxalate nephrolithiasis in a rat model. *Ren. Fail.* **2017**, *39*, 120–129. [[CrossRef](#)] [[PubMed](#)]
17. Chen, P.; Ruan, A.; Zhou, J.; Zhang, X.; Ma, Y.; Peng, H.; Yang, T.; Wang, Q. Effect of total glucosides of paeony on inflammation and degeneration of chondrocytes in osteoarthritis. *Chin. J. Tissue Eng. Res.* **2021**, *25*, 4614. [[CrossRef](#)] [[PubMed](#)]
18. Ye, H.Z.; Zheng, C.S.; Xu, X.J.; Wu, M.X.; Liu, X.X. Potential synergistic and multitarget effect of herbal pair Chuanxiong Rhizome-*Paeonia Albiflora* Pall on osteoarthritis disease: A computational pharmacology approach. *Chin. J. Integr. Med.* **2011**, *17*, 698–703. [[CrossRef](#)] [[PubMed](#)]
19. Lin, L.X.; Zheng, F.Y.; Huang, G.Z.; Li, S.X.; Liu, F.J.; Man, S.; Wu, J.R.; Li, Y.Y. Anti-arthritic-related metal bioavailability for optimal compatibility ratio of *Aconiti Radix Cocta* and *Paeoniae Radix Alba*. *Zhongguo Zhong Yao Za Zhi* **2020**, *45*, 5770–5776. [[CrossRef](#)]
20. Zhang, L.; Han, L.; Wang, X.; Wei, Y.; Zheng, J.; Zhao, L.; Tong, X. Exploring the mechanisms underlying the therapeutic effect of *Salvia miltiorrhiza* in diabetic nephropathy using network pharmacology and molecular docking. *Biosci. Rep.* **2021**, *41*, BSR20203520. [[CrossRef](#)]
21. Shaker, B.; Yu, M.S.; Lee, J.; Lee, Y.; Jung, C.; Na, D. User guide for the discovery of potential drugs via protein structure prediction and ligand docking simulation. *J. Microbiol.* **2020**, *58*, 235–244. [[CrossRef](#)] [[PubMed](#)]
22. Hopkins, A.L. Network pharmacology: The next paradigm in drug discovery. *Nat. Chem. Biol.* **2008**, *4*, 682–690. [[CrossRef](#)] [[PubMed](#)]
23. Zhang, R.; Zhu, X.; Bai, H.; Ning, K. Network Pharmacology Databases for Traditional Chinese Medicine: Review and Assessment. *Front. Pharmacol.* **2019**, *10*, 123. [[CrossRef](#)]
24. Wang, X.; Wang, Z.Y.; Zheng, J.H.; Li, S. TCM network pharmacology: A new trend towards combining computational, experimental and clinical approaches. *Chin. J. Nat. Med.* **2021**, *19*, 1–11. [[CrossRef](#)] [[PubMed](#)]
25. Luo, T.T.; Lu, Y.; Yan, S.K.; Xiao, X.; Rong, X.L.; Guo, J. Network Pharmacology in Research of Chinese Medicine Formula: Methodology, Application and Prospective. *Chin. J. Integr. Med.* **2020**, *26*, 72–80. [[CrossRef](#)] [[PubMed](#)]
26. Zhang, R.Z.; Yu, S.J.; Bai, H.; Ning, K. TCM-Mesh: The database and analytical system for network pharmacology analysis for TCM preparations. *Sci. Rep.* **2017**, *7*, 2821. [[CrossRef](#)] [[PubMed](#)]
27. Yan, B.; Shen, M.; Fang, J.; Wei, D.; Qin, L. Advancement in the chemical analysis of *Paeoniae Radix* (Shaoyao). *J. Pharm. Biomed. Anal.* **2018**, *160*, 276–288. [[CrossRef](#)]
28. Deng, H.; Yan, C.; Xiao, T.; Yuan, D.; Xu, J. Total glucosides of *Paeonia lactiflora* Pall inhibit vascular endothelial growth factor-induced angiogenesis. *J. Ethnopharmacol.* **2010**, *127*, 781–785. [[CrossRef](#)]
29. Wei, C.; Wan, L.; Wang, H.; Huang, G. Optimization of Extraction Process for *Paeoniae radix Alba* by Central Composite Design-Response Surface Methodology. *Her. Med.* **2016**, 175–177.
30. Shen, M.; Zhang, Q.; Qin, L.; Yan, B. Single Standard Substance for the Simultaneous Determination of Eleven Components in the Extract of *Paeoniae Radix Alba* (Root of *Paeonia lactiflora* Pall.). *J. Anal. Methods Chem.* **2021**, *2021*, 8860776. [[CrossRef](#)]
31. Jeon, M.H.; Kwon, H.J.; Jeong, J.S.; Lee, Y.M.; Hong, S.P. Detection of albiflorin and paeoniflorin in *Paeoniae radix* by reversed-phase high-performance liquid chromatography with pulsed amperometric detection. *J. Chromatogr. A* **2009**, *1216*, 4568–4573. [[CrossRef](#)] [[PubMed](#)]

32. Wang, R.; Peng, X.; Wang, L.; Tan, B.; Liu, J.; Feng, Y.; Yang, S. Preparative purification of peoniflorin and albiflorin from peony rhizome using macroporous resin and medium-pressure liquid chromatography. *J. Sep. Sci.* **2012**, *35*, 1985–1992. [[CrossRef](#)] [[PubMed](#)]
33. Chu, C.; Zhang, S.; Tong, S.; Li, X.; Li, Q.; Yan, J. Elution-extrusion counter-current chromatography for the separation of two pairs of isomeric monoterpenes from *Paeoniae Alba Radix*. *J. Sep. Sci.* **2015**, *38*, 3110–3118. [[CrossRef](#)] [[PubMed](#)]
34. Wu, Y.; Jiang, Y.; Zhang, L.; Zhou, J.; Yu, Y.; Zhang, S.; Zhou, Y. Green and efficient extraction of total glucosides from *Paeonia lactiflora* Pall. 'Zhongjiang' by subcritical water extraction combined with macroporous resin enrichment. *Ind. Crops Prod.* **2019**, *141*, 111699. [[CrossRef](#)]
35. Liu, E.H.; Qi, L.W.; Li, B.; Peng, Y.B.; Li, P.; Li, C.Y.; Cao, J. High-speed separation and characterization of major constituents in *Radix Paeoniae Rubra* by fast high-performance liquid chromatography coupled with diode-array detection and time-of-flight mass spectrometry. *Rapid Commun. Mass. Spectrom.* **2009**, *23*, 119–130. [[CrossRef](#)] [[PubMed](#)]
36. Wang, Y.; Wang, P.; Xu, C.; Sun, S.; Zhou, Q.; Shi, Z.; Li, J.; Chen, T.; Li, Z.; Cui, W. Discrimination and chemical characterization of different *Paeonia lactiflora* (*Radix Paeoniae Alba* and *Radix Paeoniae Rubra*) by infrared macro-fingerprint analysis-through-separation. *J. Mol. Struct.* **2015**, *1099*, 68–76. [[CrossRef](#)]
37. Medzhitov, R.; Horng, T. Transcriptional control of the inflammatory response. *Nat. Rev. Immunol.* **2009**, *9*, 692–703. [[CrossRef](#)] [[PubMed](#)]
38. Xiao, L.; Lin, S.; Zhan, F. One of the active ingredients in *Paeoniae Radix Alba* functions as JAK1 inhibitor in rheumatoid arthritis. *Front. Pharmacol.* **2022**, *13*, 906763. [[CrossRef](#)] [[PubMed](#)]
39. Sang, X.; Ying, J.; Wan, X.; Han, X.; Shan, Q.; Lyu, Q.; Yang, Q.; Wang, K.; Hao, M.; Liu, E.; et al. Screening of Bioactive Fraction of *Radix Paeoniae Alba* and Enhancing Anti-Allergic Asthma by Stir-Frying Through Regulating PI3K/AKT Signaling Pathway. *Front. Pharmacol.* **2022**, *13*, 863403. [[CrossRef](#)]
40. Li, P.P.; Liu, D.D.; Liu, Y.J.; Song, S.S.; Wang, Q.T.; Chang, Y.; Wu, Y.J.; Chen, J.Y.; Zhao, W.D.; Zhang, L.L.; et al. BAFF/BAFF-R involved in antibodies production of rats with collagen-induced arthritis via PI3K-Akt-mTOR signaling and the regulation of peoniflorin. *J. Ethnopharmacol.* **2012**, *141*, 290–300. [[CrossRef](#)]
41. Wang, T.; Zhou, X.; Kuang, G.; Jiang, R.; Guo, X.; Wu, S.; Wan, J.; Yin, L. Peoniflorin modulates oxidative stress, inflammation and hepatic stellate cells activation to alleviate CCl₄-induced hepatic fibrosis by upregulation of heme oxygenase-1 in mice. *J. Pharm. Pharmacol.* **2021**, *73*, 338–346. [[CrossRef](#)] [[PubMed](#)]
42. Qian, W.; Zhang, J.; Wang, W.; Wang, T.; Liu, M.; Yang, M.; Sun, Z.; Li, X.; Li, Y. Antimicrobial and antibiofilm activities of peoniflorin against carbapenem-resistant *Klebsiella pneumoniae*. *J. Appl. Microbiol.* **2020**, *128*, 401–413. [[CrossRef](#)] [[PubMed](#)]
43. Ho, J.Y.; Chang, H.W.; Lin, C.F.; Liu, C.J.; Hsieh, C.F.; Horng, J.T. Characterization of the anti-influenza activity of the Chinese herbal plant *Paeonia lactiflora*. *Viruses* **2014**, *6*, 1861–1875. [[CrossRef](#)] [[PubMed](#)]
44. Wang, H.; Zhou, H.; Wang, C.X.; Li, Y.S.; Xie, H.Y.; Luo, J.D.; Zhou, Y. Peoniflorin inhibits growth of human colorectal carcinoma HT 29 cells in vitro and in vivo. *Food Chem. Toxicol.* **2012**, *50*, 1560–1567. [[CrossRef](#)]
45. Zheng, M.; Liu, C.; Fan, Y.; Shi, D.; Jian, W. Total glucosides of peony (TGP) extracted from *Radix Paeoniae Alba* exerts neuroprotective effects in MPTP-induced experimental parkinsonism by regulating the cAMP/PKA/CREB signaling pathway. *J. Ethnopharmacol.* **2019**, *245*, 112182. [[CrossRef](#)] [[PubMed](#)]
46. Liu, M.; Feng, J.; Du, Q.; Ai, J.; Lv, Z. Peoniflorin Attenuates Myocardial Fibrosis in Isoprenaline-induced Chronic Heart Failure Rats via Inhibiting P38 MAPK Pathway. *Curr. Med. Sci.* **2020**, *40*, 307–312. [[CrossRef](#)] [[PubMed](#)]
47. Jiang, D.; Chen, Y.; Hou, X.; Xu, J.; Mu, X.; Chen, W. Influence of *Paeonia lactiflora* roots extract on cAMP-phosphodiesterase activity and related anti-inflammatory action. *J. Ethnopharmacol.* **2011**, *137*, 914–920. [[CrossRef](#)] [[PubMed](#)]
48. Liao, T.; Kang, J.; Ma, Z.; Jie, L.; Feng, M.; Liu, D.; Mao, J.; Wang, P.; Xing, R. Total glucosides of white peony capsule alleviate articular cartilage degeneration and aberrant subchondral bone remodeling in knee osteoarthritis. *Phytother. Res.* **2024**. [[CrossRef](#)] [[PubMed](#)]
49. Hu, P.F.; Sun, F.F.; Jiang, L.F.; Bao, J.P.; Wu, L.D. Peoniflorin inhibits IL-1 β -induced MMP secretion via the NF- κ B pathway in chondrocytes. *Exp. Ther. Med.* **2018**, *16*, 1513–1519. [[CrossRef](#)]
50. Hu, P.F.; Chen, W.P.; Bao, J.P.; Wu, L.D. Peoniflorin inhibits IL-1 β -induced chondrocyte apoptosis by regulating the Bax/Bcl-2/caspase-3 signaling pathway. *Mol. Med. Rep.* **2018**, *17*, 6194–6200. [[CrossRef](#)]
51. Wu, L.; Tang, R.; Xiong, W.; Song, S.; Guo, Q.; Zhang, Q. Peoniflorin shows chondroprotective effects under IL-1 β stress by regulating circ-PREX1/miR-140-3p/WNT5B axis. *J. Orthop. Surg. Res.* **2023**, *18*, 766. [[CrossRef](#)] [[PubMed](#)]
52. Zhao, L.; Chang, Q.; Huang, T.; Huang, C. Peoniflorin inhibits IL-1 β -induced expression of inflammatory mediators in human osteoarthritic chondrocyte. *Mol. Med. Rep.* **2018**, *17*, 3306–3311. [[CrossRef](#)] [[PubMed](#)]
53. Chao Wei, C.; Yi Shan, D.; Fei Yue, L.; Tian You, F. Total Glucosides of Peony Alleviate Joint Destruction in Rabbits with Osteoarthritis. *Nat. Prod. Commun.* **2023**, *18*, 1934578X231192211. [[CrossRef](#)]
54. Ahmad, M.; Malik, K.; Tariq, A.; Zhang, G.; Yaseen, G.; Rashid, N.; Sultana, S.; Zafar, M.; Ullah, K.; Khan, M.P.Z. Botany, ethnomedicines, phytochemistry and pharmacology of Himalayan peony (*Paeonia emodi* Royle.). *J. Ethnopharmacol.* **2018**, *220*, 197–219. [[CrossRef](#)] [[PubMed](#)]
55. Luo, J.; Jin, D.E.; Yang, G.Y.; Zhang, Y.Z.; Wang, J.M.; Kong, W.P.; Tao, Q.W. Total glucosides of peony for rheumatoid arthritis: A systematic review of randomized controlled trials. *Complement. Ther. Med.* **2017**, *34*, 46–56. [[CrossRef](#)] [[PubMed](#)]

56. Martel-Pelletier, J.; Barr, A.J.; Cicuttini, F.M.; Conaghan, P.G.; Cooper, C.; Goldring, M.B.; Goldring, S.R.; Jones, G.; Teichtahl, A.J.; Pelletier, J.-P. Osteoarthritis. *Nat. Rev. Dis. Primers* **2016**, *13*, 16072. [[CrossRef](#)] [[PubMed](#)]
57. Krustev, E.; Rioux, D.; McDougall, J.J. Mechanisms and mediators that drive arthritis pain. *Curr. Osteoporos. Rep.* **2015**, *13*, 216–224. [[CrossRef](#)] [[PubMed](#)]
58. Huang, H.; Lou, Z.; Zheng, S.; Wu, J.; Yao, Q.; Chen, R.; Kou, L.; Chen, D. Intra-articular drug delivery systems for osteoarthritis therapy: Shifting from sustained release to enhancing penetration into cartilage. *Drug Deliv.* **2022**, *29*, 767–791. [[CrossRef](#)] [[PubMed](#)]
59. Zhong, W.; Chen, J.; Li, Y.; Liu, M.; Yang, S. Efficacy and safety of traditional Chinese medicine rehabilitation program in the treatment of knee osteoarthritis: A randomized controlled trial protocol. *Ann. Palliat. Med.* **2021**, *10*, 6909–6918. [[CrossRef](#)]
60. Molnar, V.; Matišić, V.; Kodvanj, I.; Bjelica, R.; Jeleč, Ž.; Hudetz, D.; Rod, E.; Čukelj, F.; Vrdoljak, T.; Vidović, D. Cytokines and chemokines involved in osteoarthritis pathogenesis. *Int. J. Mol. Sci.* **2021**, *22*, 9208. [[CrossRef](#)]
61. Robinson, W.H.; Lepus, C.M.; Wang, Q.; Raghu, H.; Mao, R.; Lindstrom, T.M.; Sokolove, J. Low-grade inflammation as a key mediator of the pathogenesis of osteoarthritis. *Nat. Rev. Rheumatol.* **2016**, *12*, 580–592. [[CrossRef](#)]
62. Zhang, W.; Li, P.; Song, D.; Niu, H.; Shi, S.; Wang, S.; Duan, J. Structural characterization and biological activities of two α -glucans from *Radix Paeoniae Alba*. *Glycoconj. J.* **2016**, *33*, 147–157. [[CrossRef](#)] [[PubMed](#)]
63. Chen, C.; Yin, Q.; Tian, J.; Gao, X.; Qin, X.; Du, G.; Zhou, Y. Studies on the Changes of Pharmacokinetics Behaviors of Phytochemicals and the Influence on Endogenous Metabolites After the Combination of *Radix Bupleuri* and *Radix Paeoniae Alba* Based on Multi-Component Pharmacokinetics and Metabolomics. *Front. Pharmacol.* **2021**, *12*, 630970. [[CrossRef](#)] [[PubMed](#)]
64. Zhao, S.; Li, S. Network-based relating pharmacological and genomic spaces for drug target identification. *PLoS ONE* **2010**, *5*, e11764. [[CrossRef](#)]
65. Lee, W.S.; Lee, E.G.; Sung, M.S.; Yoo, W.H. Kaempferol inhibits IL-1 β -stimulated, RANKL-mediated osteoclastogenesis via downregulation of MAPKs, c-Fos, and NFATc1. *Inflammation* **2014**, *37*, 1221–1230. [[CrossRef](#)]
66. Zhuang, Z.; Ye, G.; Huang, B. Kaempferol alleviates the interleukin-1 β -induced inflammation in rat osteoarthritis chondrocytes via suppression of NF- κ B. *Med. Sci. Monit. Int. Med. J. Exp. Clin. Res.* **2017**, *23*, 3925. [[CrossRef](#)]
67. Jiang, R.; Hao, P.; Yu, G.; Liu, C.; Yu, C.; Huang, Y.; Wang, Y. Kaempferol protects chondrogenic ATDC5 cells against inflammatory injury triggered by lipopolysaccharide through down-regulating miR-146a. *Int. Immunopharmacol.* **2019**, *69*, 373–381. [[CrossRef](#)]
68. Yimam, M.; Lee, Y.-C.; Jiao, P.; Hong, M.; Nam, J.-B.; Brownell, L.; Hyun, E.; Jia, Q. UP1306, a botanical composition with analgesic and anti-inflammatory effect. *Pharmacogn. Res.* **2016**, *8*, 186. [[CrossRef](#)]
69. Du, W.; Liang, X.; Wang, S.; Lee, P.; Zhang, Y. The underlying mechanism of *Paeonia lactiflora* Pall. in Parkinson's disease based on a network pharmacology approach. *Front. Pharmacol.* **2020**, *11*, 581984. [[CrossRef](#)]
70. Fang, H.; Beier, F. Mouse models of osteoarthritis: Modelling risk factors and assessing outcomes. *Nat. Rev. Rheumatol.* **2014**, *10*, 413–421. [[CrossRef](#)]
71. Gu, R.; Liu, N.; Luo, S.; Huang, W.; Zha, Z.; Yang, J. MicroRNA-9 regulates the development of knee osteoarthritis through the NF-kappaB1 pathway in chondrocytes. *Medicine* **2016**, *95*, e4315. [[CrossRef](#)] [[PubMed](#)]
72. Lu, J.; Zhang, H.; Pan, J.; Hu, Z.; Liu, L.; Liu, Y.; Yu, X.; Bai, X.; Cai, D.; Zhang, H. Fargesin ameliorates osteoarthritis via macrophage reprogramming by downregulating MAPK and NF- κ B pathways. *Arthritis Res. Ther.* **2021**, *23*, 142. [[CrossRef](#)] [[PubMed](#)]
73. Jha, B.; Jza, B.; Jwa, B.; Quan, C.; Wd, D.; Ffa, B.; Hya, B.; Sya, B.; Hjab, C.; Ptab, E. Loganin ameliorates cartilage degeneration and osteoarthritis development in an osteoarthritis mouse model through inhibition of NF- κ B activity and pyroptosis in chondrocytes. *J. Ethnopharmacol.* **2020**, *247*, 112261. [[CrossRef](#)] [[PubMed](#)]
74. Gao, H.; Peng, L.; Li, C.; Ji, Q.; Li, P. Salidroside Alleviates Cartilage Degeneration Through NF- κ B Pathway in Osteoarthritis Rats. *Drug Des. Dev. Ther.* **2020**, *14*, 1445–1454. [[CrossRef](#)] [[PubMed](#)]
75. McGettrick, A.F.; O'Neill, L.A.J. The Role of HIF in Immunity and Inflammation. *Cell Metab.* **2020**, *32*, 524–536. [[CrossRef](#)] [[PubMed](#)]
76. Yudoh, K.; Nakamura, H.; Masukohongo, K.; Kato, T.; Nishioka, K. Catabolic stress induces expression of hypoxiainducible factor (HIF)-1 α in articular chondrocytes: Involvement of HIF-1 α in the pathogenesis of osteoarthritis. *Arthritis Res. Ther.* **2005**, *7*, 225. [[CrossRef](#)]
77. Pf, D.; Swoboda, B.; Cramer, T. Commentary The role of HIF-1 α in maintaining cartilage homeostasis and during the pathogenesis of osteoarthritis. *Arthritis Res. Ther.* **2006**, *8*, 104. [[CrossRef](#)]
78. Chang, J.; Jackson, S.G.; Wardale, J.; Jones, S.W. Hypoxia Modulates the Phenotype of Osteoblasts Isolated From Knee Osteoarthritis Patients, Leading to Undermineralized Bone Nodule Formation. *Arthritis Rheum.* **2014**, *66*, 1789–1799. [[CrossRef](#)]
79. Hu, S.; Zhang, C.; Ni, L.; Huang, C.; Chen, D.; Shi, K.; Jin, H.; Zhang, K.; Li, Y.; Xie, L. Stabilization of HIF-1 α alleviates osteoarthritis via enhancing mitophagy. *Cell Death Dis.* **2020**, *11*, 481. [[CrossRef](#)]
80. Hamilton, J.L.; Nagao, M.; Levine, B.R.; Chen, D.; Olsen, B.R.; Im, H.J. Targeting VEGF and Its Receptors for the Treatment of Osteoarthritis and Associated Pain. *J. Bone Min. Res.* **2016**, *31*, 911–924. [[CrossRef](#)]
81. Qian, J.J.; Xu, Q.; Xu, W.M.; Cai, R.; Huang, G.C. Expression of VEGF-A Signaling Pathway in Cartilage of ACLT-induced Osteoarthritis Mouse Model. *J. Orthop. Surg. Res.* **2021**, *16*, 379. [[CrossRef](#)] [[PubMed](#)]

82. Wang, Y.H.; Kuo, S.J.; Liu, S.C.; Wang, S.W.; Tsai, C.H.; Fong, Y.C.; Tang, C.H. Apelin Affects the Progression of Osteoarthritis by Regulating VEGF-Dependent Angiogenesis and miR-150-5p Expression in Human Synovial Fibroblasts. *Cells* **2020**, *9*, 594. [[CrossRef](#)] [[PubMed](#)]
83. Su, L.; Wang, Y.; Bao, Y.; Liu, X.; Xu, H. LncRNA MEG3 promotes recovery of knee osteoarthritis in rats through regulating VEGF expression. *Panminerva Med.* **2020**. [[CrossRef](#)] [[PubMed](#)]
84. Ru, J.; Li, P.; Wang, J.; Zhou, W.; Li, B.; Huang, C.; Li, P.; Guo, Z.; Tao, W.; Yang, Y.; et al. TCMSP: A database of systems pharmacology for drug discovery from herbal medicines. *J. Cheminform* **2014**, *6*, 13. [[CrossRef](#)] [[PubMed](#)]
85. Wishart, D.S.; Knox, C.; Guo, A.C.; Shrivastava, S.; Hassanali, M.; Stothard, P.; Chang, Z.; Woolsey, J. DrugBank: A comprehensive resource for in silico drug discovery and exploration. *Nucleic Acids Res.* **2006**, *34*, D668–D672. [[CrossRef](#)] [[PubMed](#)]
86. Wang, Y.; Xiao, J.; Suzek, T.O.; Zhang, J.; Wang, J.; Bryant, S.H. PubChem: A public information system for analyzing bioactivities of small molecules. *Nucleic Acids Res.* **2009**, *37*, W623–W633. [[CrossRef](#)] [[PubMed](#)]
87. Szklarczyk, D.; Franceschini, A.; Wyder, S.; Forslund, K.; Heller, D.; Huerta-Cepas, J.; Simonovic, M.; Roth, A.; Santos, A.; Tsafou, K.P.; et al. STRING v10: Protein-protein interaction networks, integrated over the tree of life. *Nucleic Acids Res.* **2015**, *43*, D447–D452. [[CrossRef](#)] [[PubMed](#)]
88. Hamosh, A.; Scott, A.F.; Amberger, J.S.; Bocchini, C.A.; McKusick, V.A. Online Mendelian Inheritance in Man (OMIM), a knowledgebase of human genes and genetic disorders. *Nucleic Acids Res.* **2005**, *33*, D514–D517. [[CrossRef](#)]
89. Qiu, J. Traditional medicine: A culture in the balance. *Nature* **2007**, *448*, 126–128. [[CrossRef](#)]

Disclaimer/Publisher’s Note: The statements, opinions and data contained in all publications are solely those of the individual author(s) and contributor(s) and not of MDPI and/or the editor(s). MDPI and/or the editor(s) disclaim responsibility for any injury to people or property resulting from any ideas, methods, instructions or products referred to in the content.